Lecture 19

Microwave detection
Inverse problems

Square-law detectors, mixers

Dicke switch

Discovery of the cosmic microwave background

Systematic errors

COBE, WMAP, PLANCK

Inverse problems

A detector for every wavelength

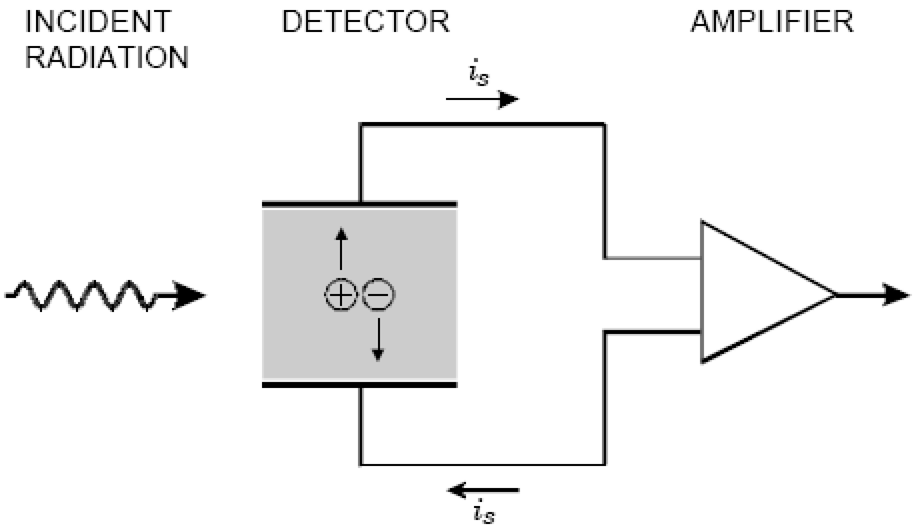

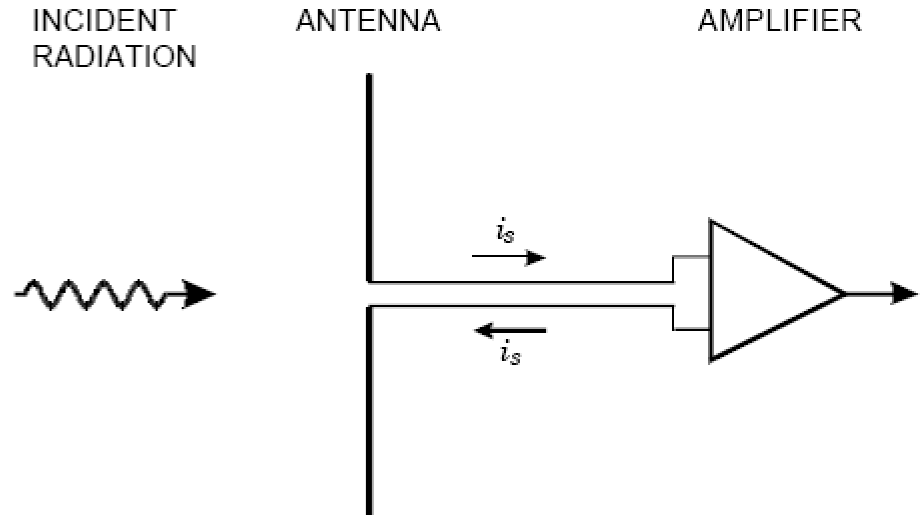

The optimal detector system depends on coupling to the detector, bandwidth, and system noise. Consider diffraction. What happens in a system with a 10 micron pixel as the wavelength approaches 5 microns?

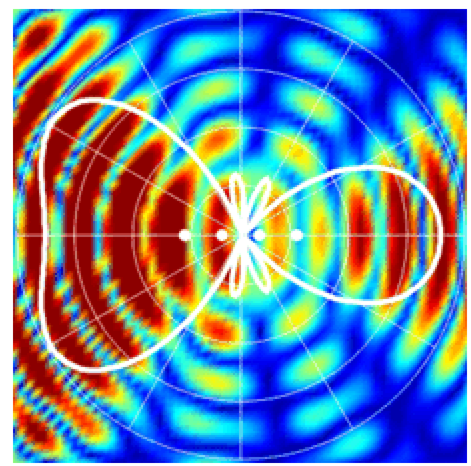

mm wavelengths: low sidelobe horn antennas

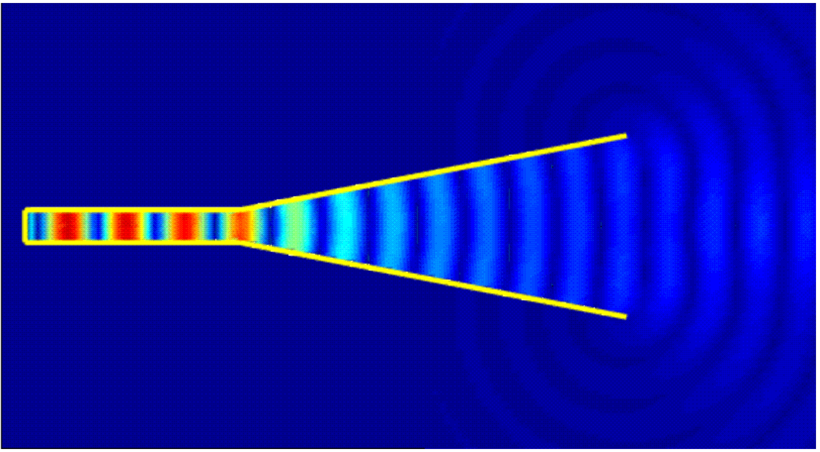

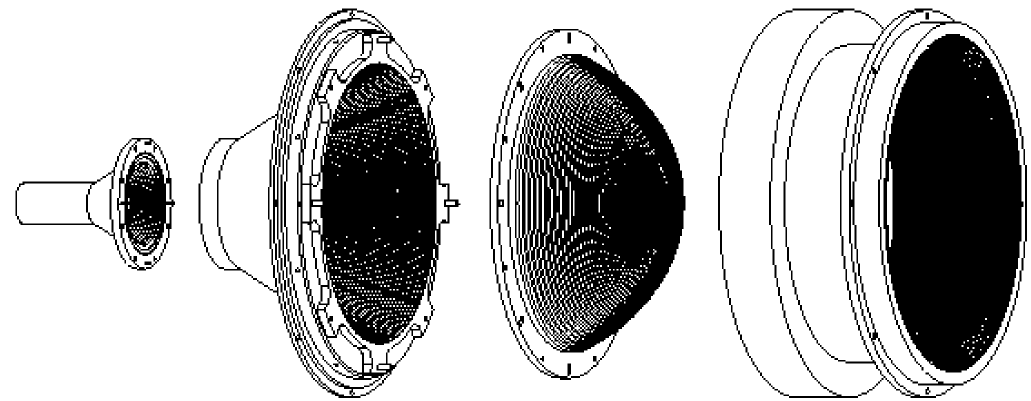

A corrugated horn produces an aperture electric field in which the fields are nearly linear. A linear electric field cannot be produced by waveguides which support pure transverse-electric (TE) or transverse-magnetic (TM) modes since they have aperture electric fields in which the field lines are curved. Only a ' balanced hybrid' mode can produce the desired linear aperture field. This happens when both the axial magnetic field and the azimuthal electric field at the edge of the corrugations are zero. The former is produced by an open circuit condition with a quarter wavelength deep corrugations and the latter by a short-circuit with many corrugations per wavelength.

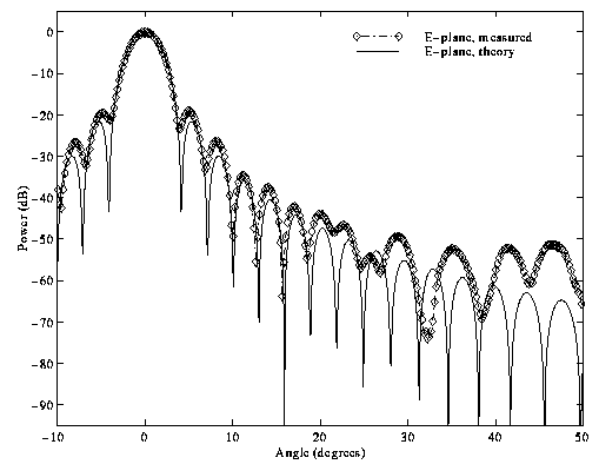

Where do you put the gain?

At the output of the detection system we need to have volt-level signals. But the signals on the input are nanovolt typically. As the signal wavelength gets longer it becomes possible to have amplification before detection. The choice of whether to detect first and amplify or to amplify and then detect is based on S/N considerations. Amplifiers have noise, and at very short wavelengths it is better to detect first (just like we did at optical wavelengths with CCDs etc).

For a multi-stage system the first stage dominates the S/N ratio.
For example, in a hetrodyne receiver the mixer noise and the IF noise combine:

$$T_R = T_{Mix} + T_{IF} / \eta$$

where η is the transfer function or conversion gain of the mixer.

Square law detector

Any AC signal can be demodulated by a nonlinear device. The bolometer is a square law detector in the quantum sense that the probability of absorbing a photon is proportional to the square of the electric field $\sim E^2$

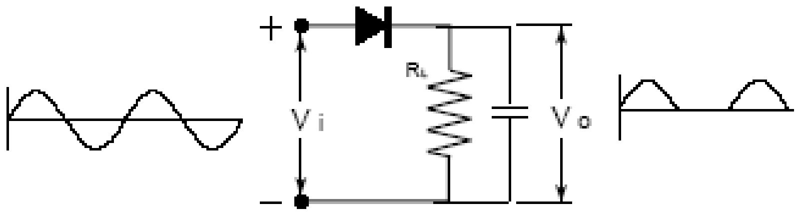

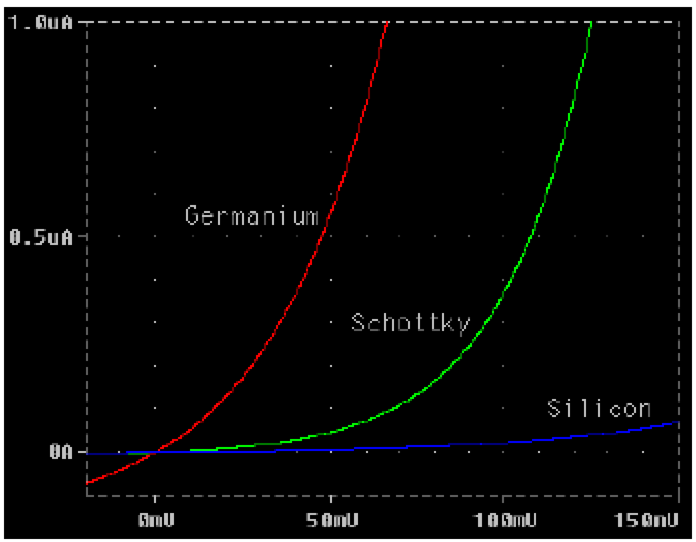

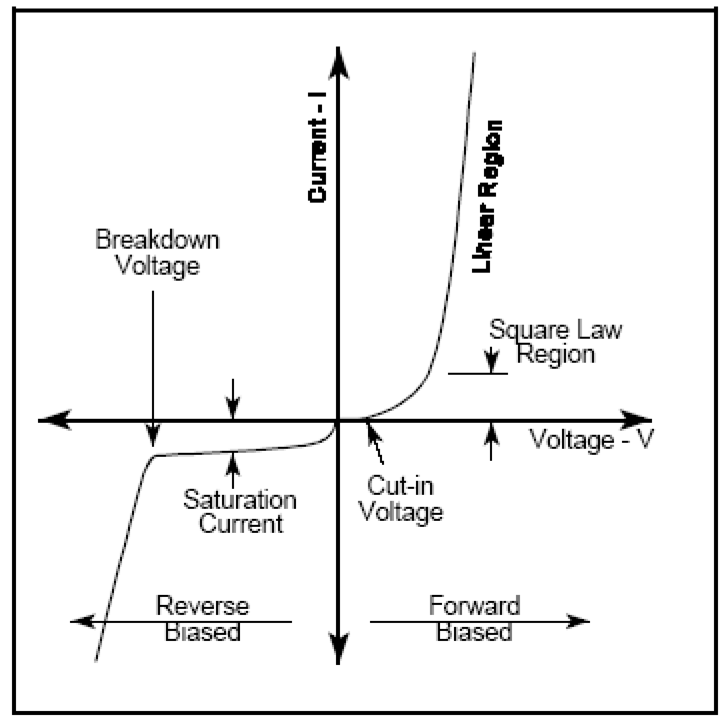

$$V_o = nV_i^2 = nP_i \quad \text{or} \quad P_i \propto V_o$$

SIS junctions are even more non-linear, as well as less noisy.

mixer

$$V_o = [A_1 \cos(\omega_1 t)][A_2 \cos(\omega_2 t)] = \frac{A_1 A_2}{2}[\cos(\omega_1 - \omega_2)t + \cos(\omega_1 + \omega_2)t]$$

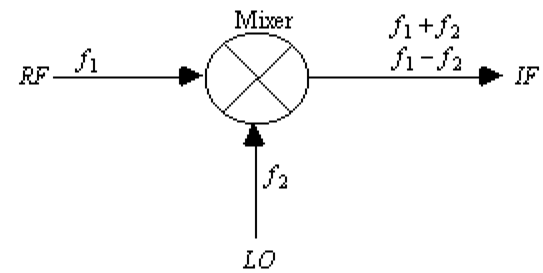

hetrodyne receiver

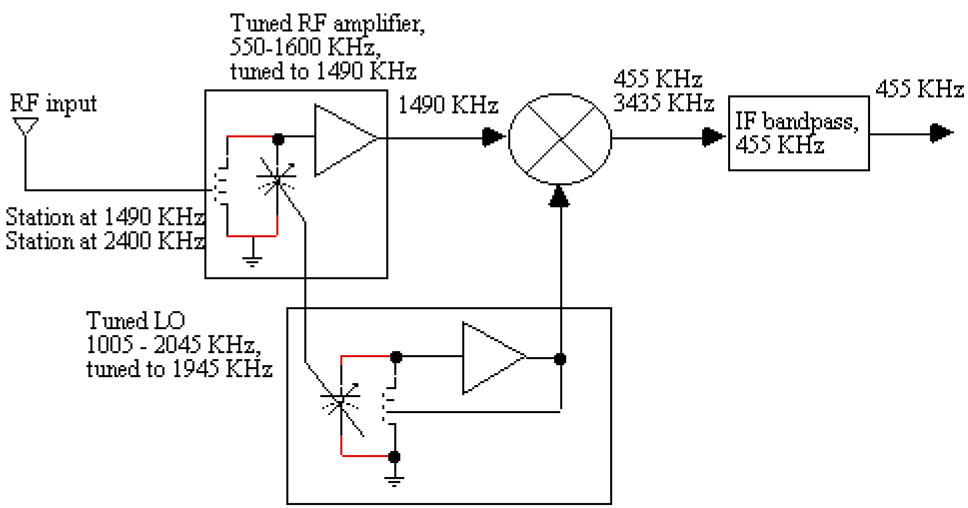

Balanced mixer

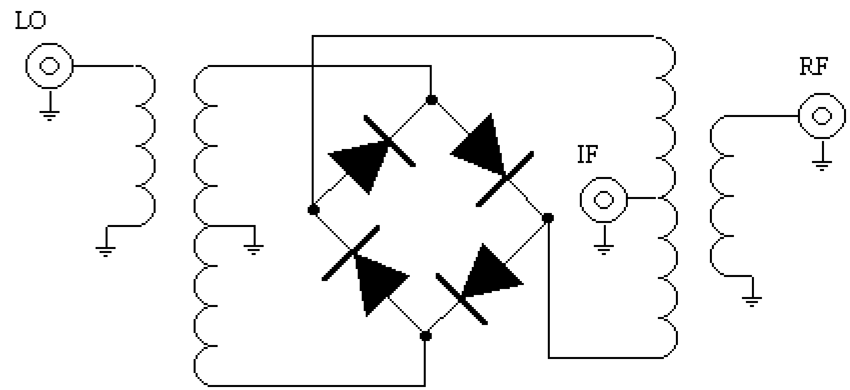

radio interferometry

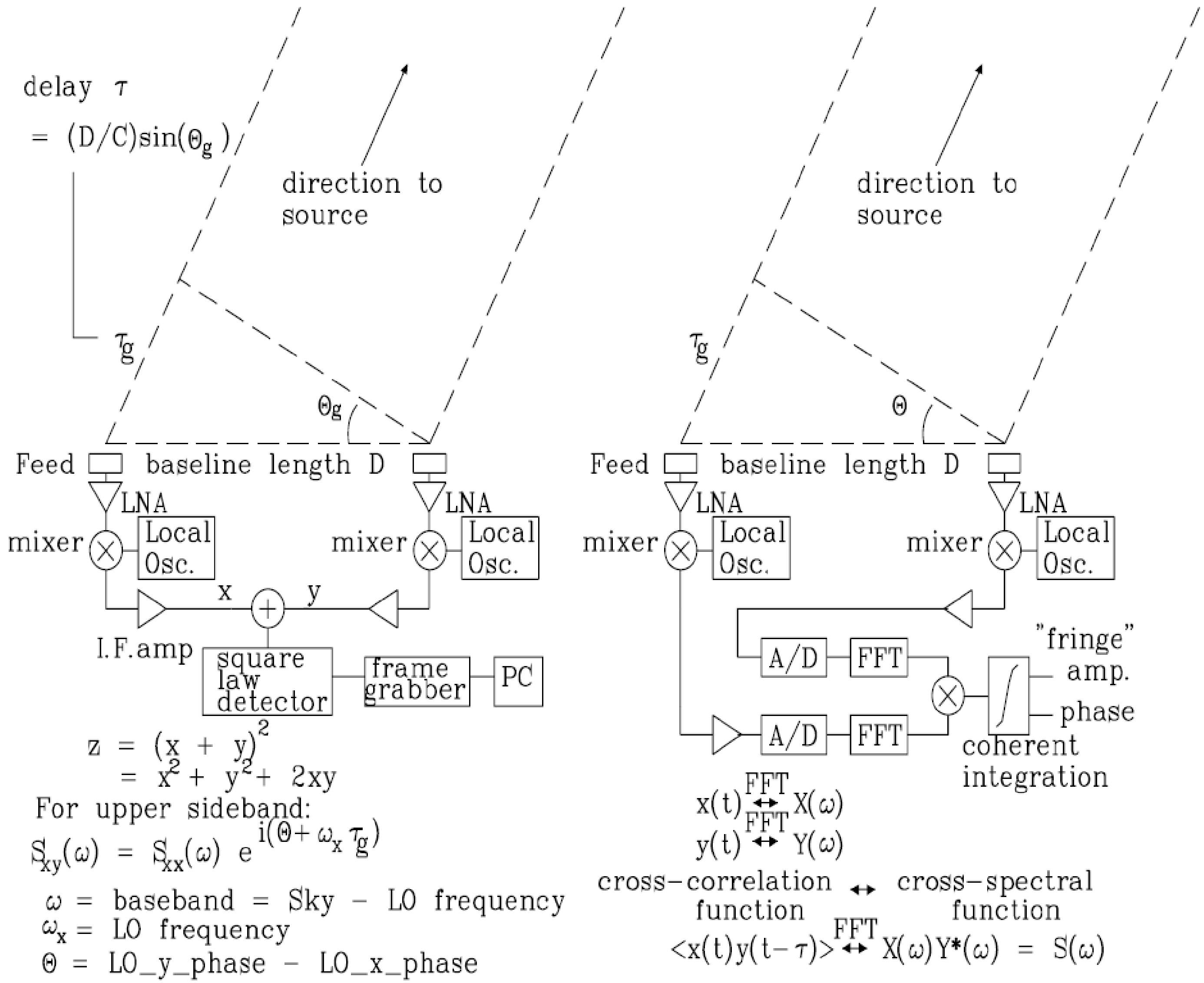

Why heterodyne?

Many receivers used in radio astronomy (all receivers used for spectroscopy) employ so-called superheterodyne schemes. The goal is to transform the frequency of the signal (SF) down to a lower frequency, called the intermediate frequency (IF) that is easier to process but without losing any of the information to be measured. This is accomplished by mixing the SF from the low noise amplifier with a local oscillator (LO) and filtering out any unwanted sidebands in the IF. A bonus is that the SF can be shifted around in the IF, or alternatively, the IF for a given SF can be shifted around by shifting the LO frequency.

Used for detection of radio line emission.

Why square-law detectors?

Inside radio-astronomy receivers, a signal is usually represented by a voltage proportional to the electric field (as collected by the antenna). But we often want to measure power or power density. So, at least for continuum measurements and for calibration, we need a device that produces an output proportional to the square of the voltage, a so-called square-law detector, and also averages over at least a few cycles of the waveform.

Used for detection of radio noise.

Noise in square law detectors

There are two bandwidths of interest: The noise bandwidth B1 before detection which is usually set by some bandpass filter and the bandwidth B2 after detection which is usually set by a low-pass filter.

What do we get when we square a noise voltage? The output comes from noise in B1 mixing with some other frequency in B2. The output noise depends on the product B1 x B2:

$$<\Delta I>^2 = 2\, a\, S_\nu \; B1\, B2 \qquad\qquad NEP = k\, T_N\, (2\, B1)^{1/2}$$

Consider a system with a HEMT amplifier into a bandpass B1 followed by square law detection and a low pass filter B2. The output is proportional to the noise power kT_N B1, where T_N is the receiver noise. This is calibrated in temperature units. The fractional error

$$\boxed{\Delta T_{rms} \,/\, T_N = (B1\, \tau)^{-1/2}}$$

This is the Dicke radiometer formula. Bob Dicke used a switch to measure and subtract T_N, so ΔT_{rms} became the accuracy with which he could measure the sky. One gets ΔT = 0.1 mK in t = 1 sec for a HEMT receiver with B1 = 10 GHz and T_N = 10 deg K.

Dicke microwave radiometer: when the signal is noise

Challenge: accurately measure microwave noise in the presence of broadband detector system noise. The microwave noise (the signal) and the system noise are both wideband and stochastic.

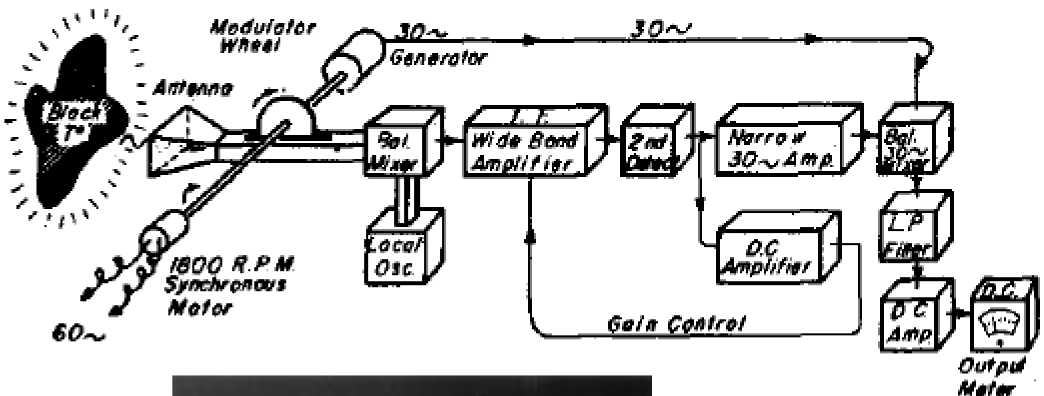

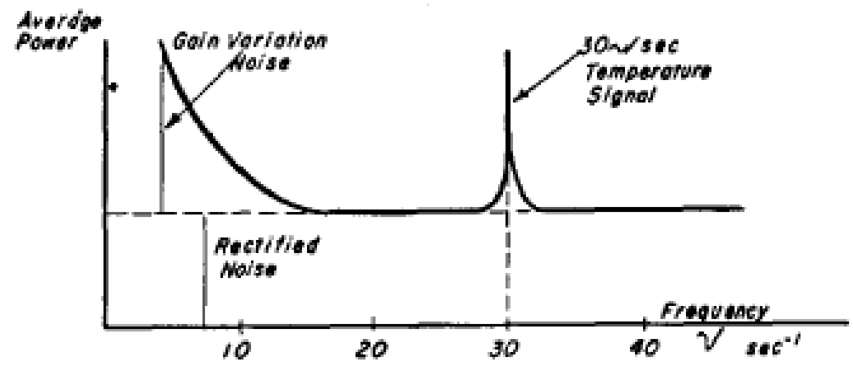

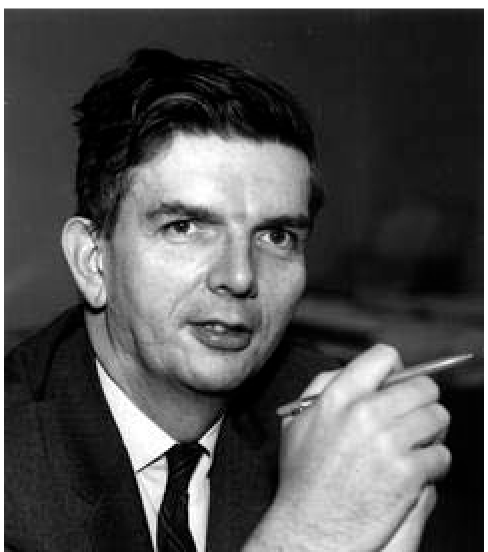

THE REVIEW OF SCIENTIFIC INSTRUMENTS VOLUME 17, NUMBER 7 JULY, 1946

The Measurement of Thermal Radiation at Microwave Frequencies

R. H. Dicke*
*Radiation Laboratory, Massachusetts Institute of Technology, Cambridge, Massachusetts***

(Received April 15, 1946)

The connection between Johnson noise and blackbody radiation is discussed, using a simple thermodynamic model. A microwave radiometer is described together with its theory of operation. The experimentally measured root mean square fluctuation of the output meter of a microwave radiometer (0.4°C) compares favorably with a theoretical value of 0.46°C. With an r-f band width of 16 mc/sec., the 0.4°C corresponds to a minimum detectable power of 10^{-16} watt. The method of calibrating using a variable temperature resistive load is described.

Dicke switch

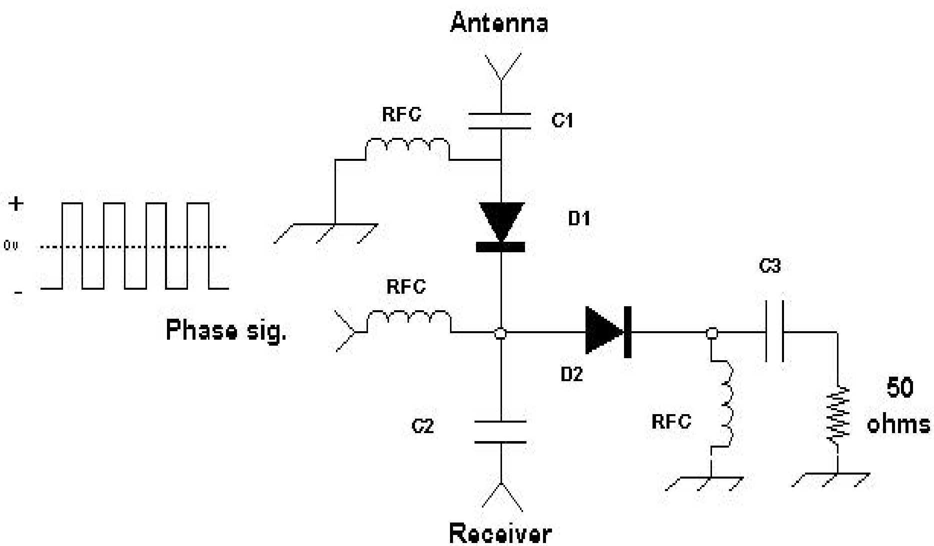

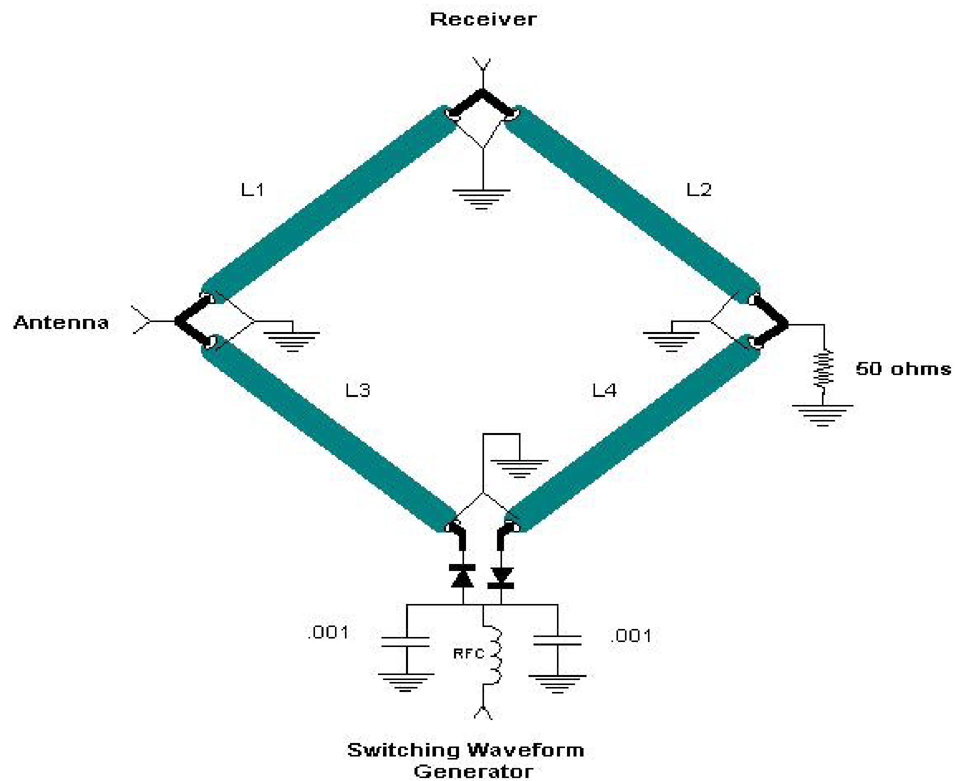

President addresses world from space

New York Herald Tribune,
13 August 1960

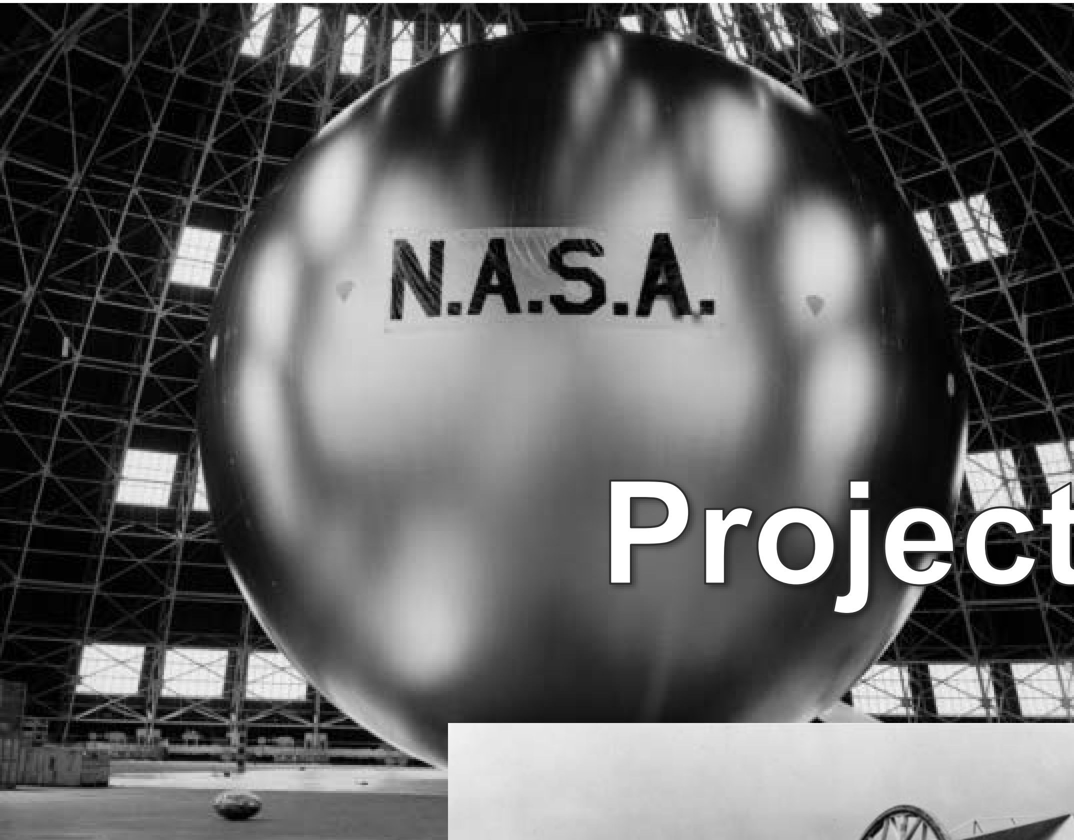

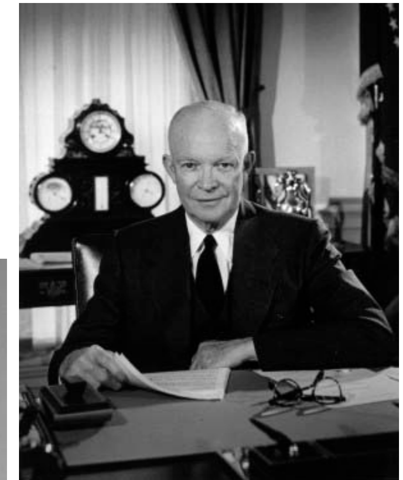

Project Echo

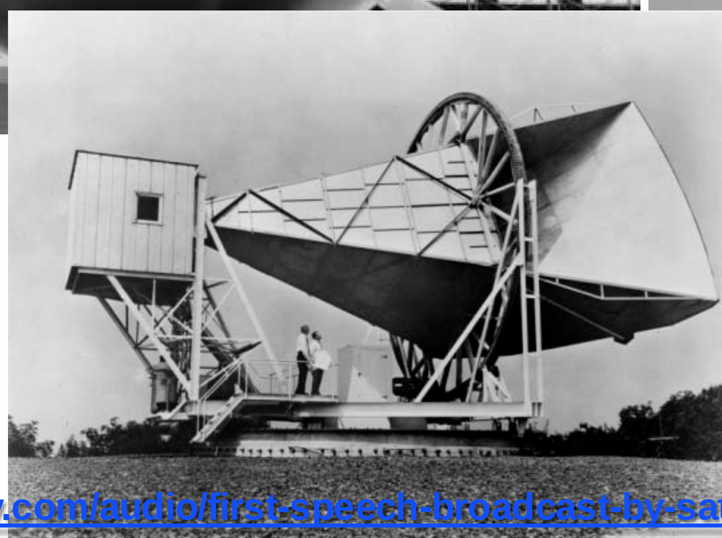

http://www.history.com/audio/first-speech-broadcast-by-satellite#first-speech-broadcast-by-satellite

A microwave system at Bell Labs with low antenna side-lobes

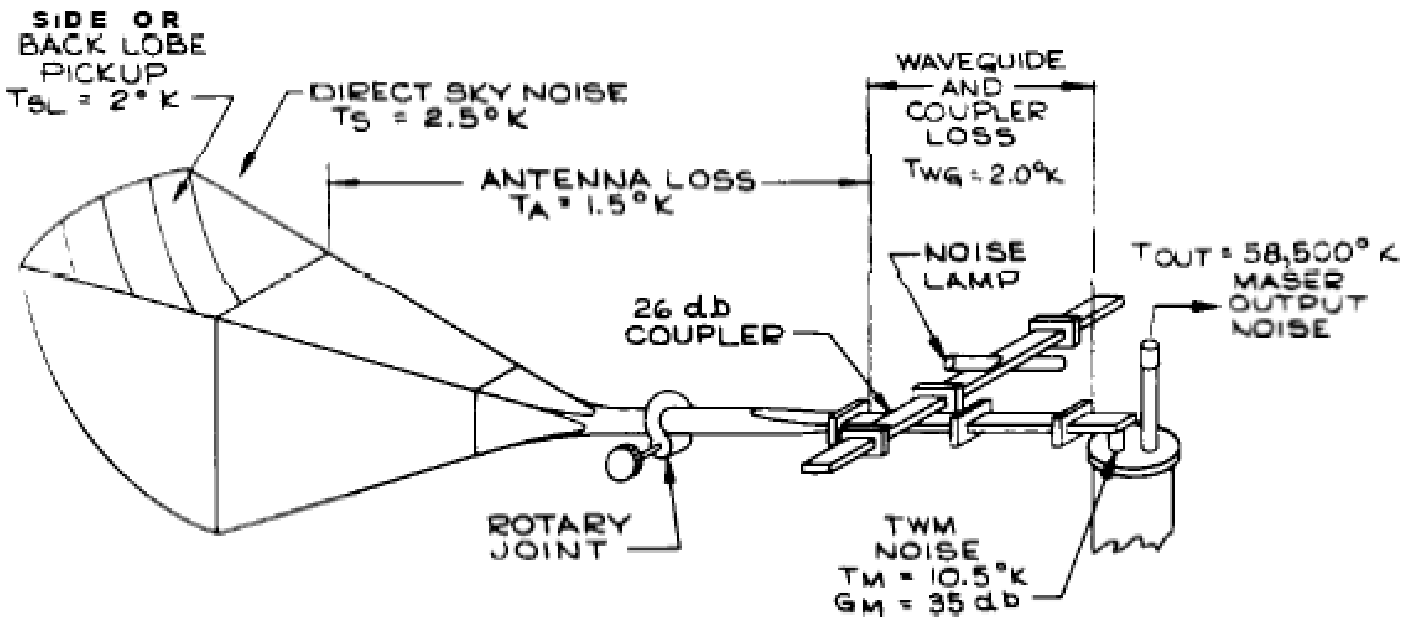

Fig. 6 A diagram of the low noise receiver used by deGrasse, Hogg, Ohm and Scovil to show that very low noise earth stations are possible. Each component is labeled with its contribution to the system noise.

CMB Discovery missed

TABLE II — SOURCES OF SYSTEM TEMPERATURE

Source	Temperature
Sky (at zenith)	$2.30 \pm 0.20°K$
Horn antenna	$2.00 \pm 1.00°K$
Waveguide (counter-clockwise channel)	$7.00 \pm 0.65°K$
Maser assembly	$7.00 \pm 1.00°K$
Converter	$0.60 \pm 0.15°K$
Predicted total system temperature	$18.90 \pm 3.00°K$

the temperature was found to vary a few degrees from day to day, but the lowest temperature was consistently $22.2 \pm 2.2°K$. By realistically assuming that all sources were then contributing their fair share (as is also tacitly assumed in Table II) it is possible to improve the over-all accuracy. The actual system temperature must be in the overlap region of the measured results and the total results of Table II, namely between 20 and 21.9°K. The most likely minimum system temperature was therefore

$$T_{system} = 21 \pm 1°K.^*$$

The inference from this result is that the "+" temperature possibilities of Table II must predominate.

Fig. 8 An excerpt from E. A. Ohm's article on the Echo receiver showing that his system temperature was 3.3K higher than predicted

Post Project Echo, two astronomers were hired: Arno Penzias and Bob Wilson

Discovery of the CMB

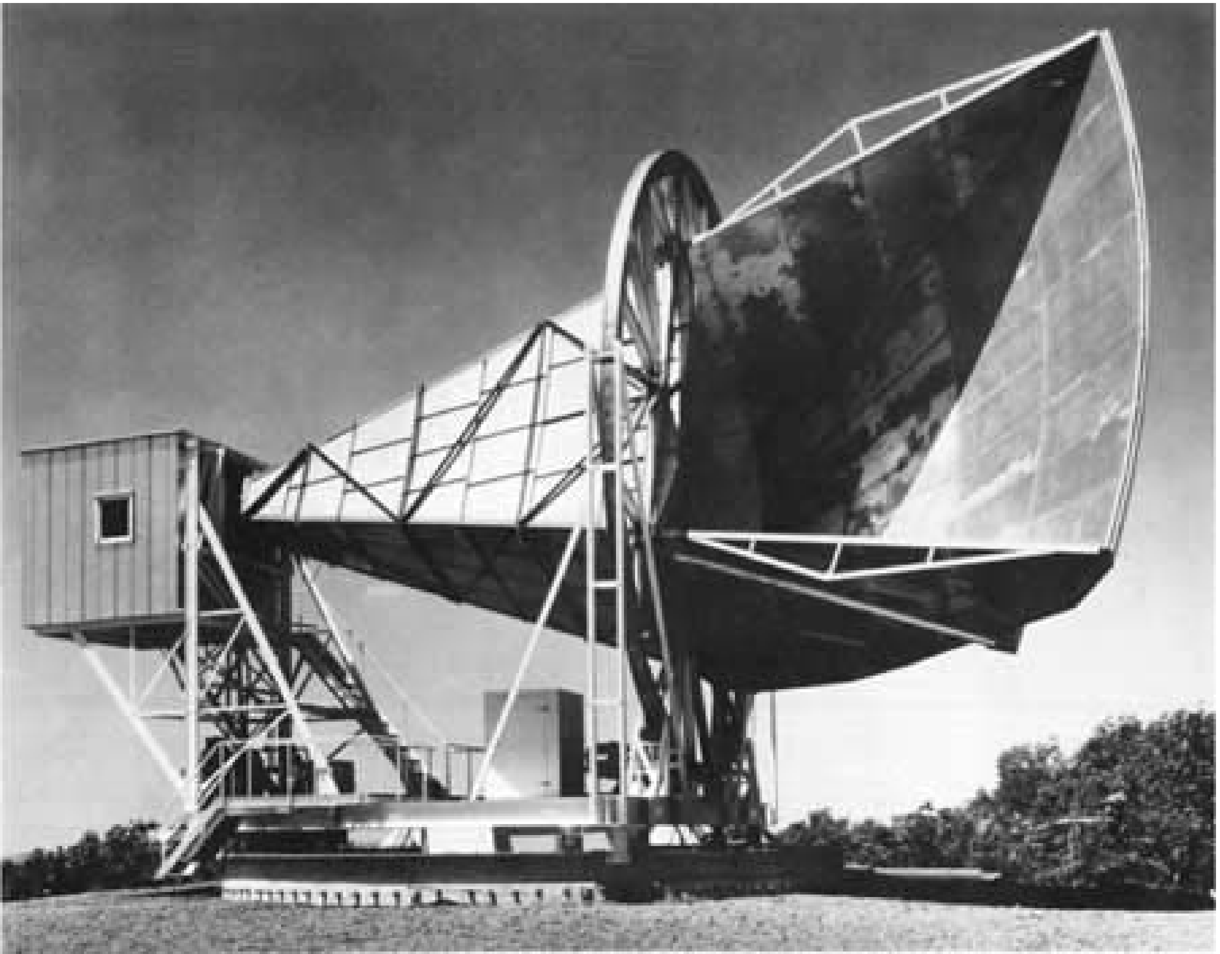

Chop between sky and a cold load:

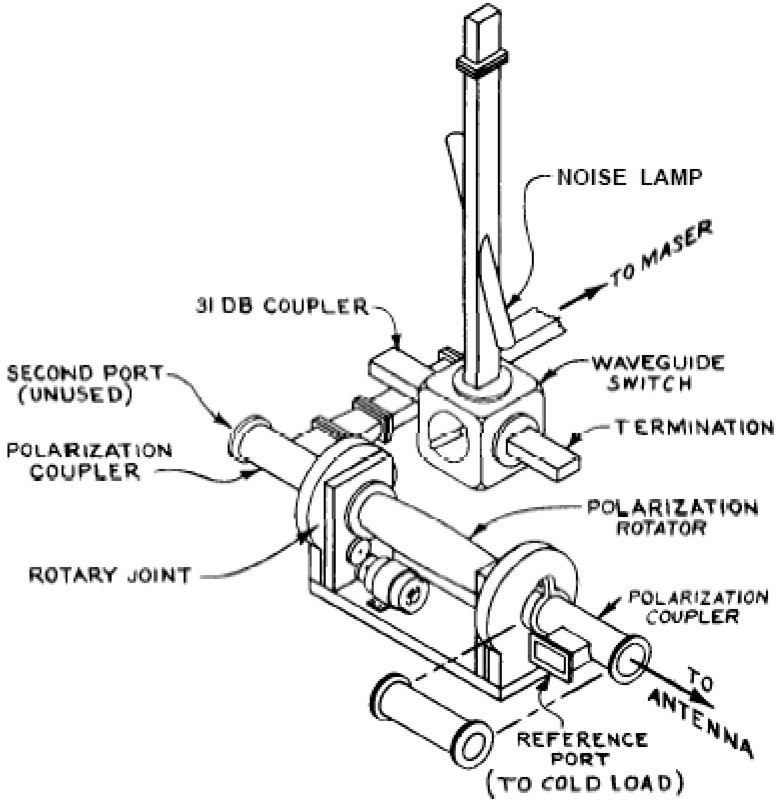

Chart recording

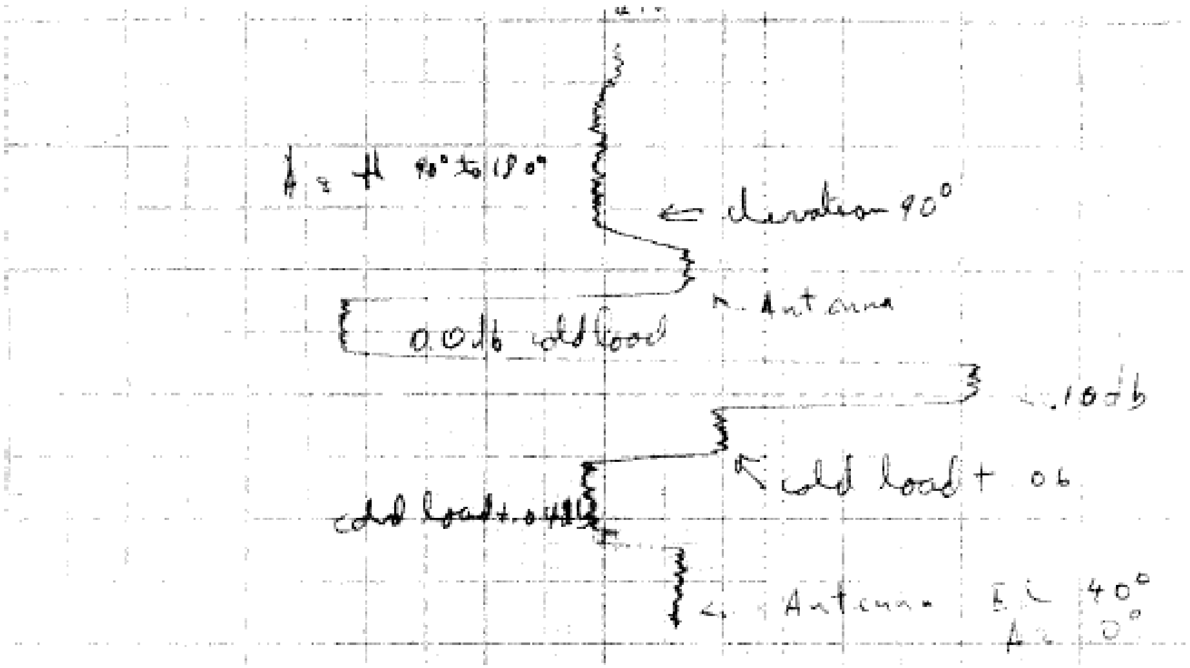

Fig. 9 The first measurement which clearly showed the presence of the microwave background. Noise temperature is plotted increasing to the right. At the top, the antenna pointed at 90° elevation is seen to have the samt noise temperature as the cold load with 0.04 db attenuation (about 7.5K). This is considerably above the expected value of 3.3K.

ApJ Letters 142, 419-421 (1965)

A MEASUREMENT OF EXCESS ANTENNA TEMPERATURE AT 4080 Mc/s

Measurements of the effective zenith noise temperature of the 20-foot horn-reflector antenna (Crawford, Hogg, and Hunt 1961) at the Crawford Hill Laboratory, Holmdel, New Jersey, at 4080 Mc/s have yielded a value about 3.5° K higher than expected. This excess temperature is, within the limits of our observations, isotropic, unpolarized, and free from seasonal variations (July, 1964–April, 1965). A possible explanation for the observed excess noise temperature is the one given by Dicke, Peebles, Roll, and Wilkinson (1965) in a companion letter in this issue.

A. A. Penzias
R. W. Wilson

May 13, 1965

Bell Telephone Laboratories, Inc
Crawford Hill, Holmdel, New Jersey

Microwave Radiometer in U2: detection of CMB dipole

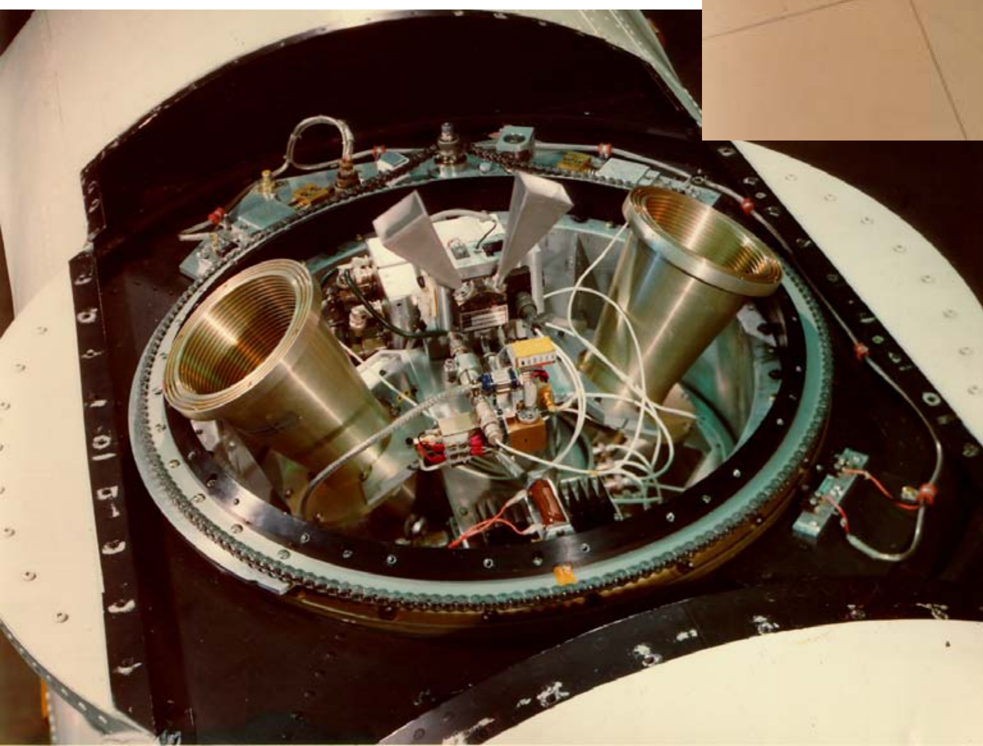

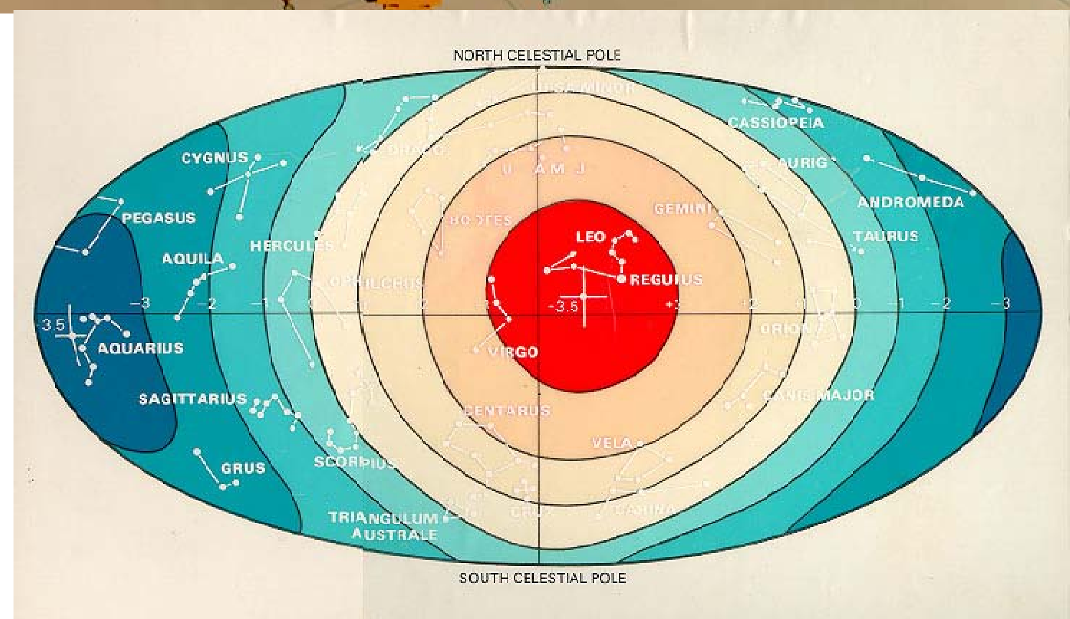

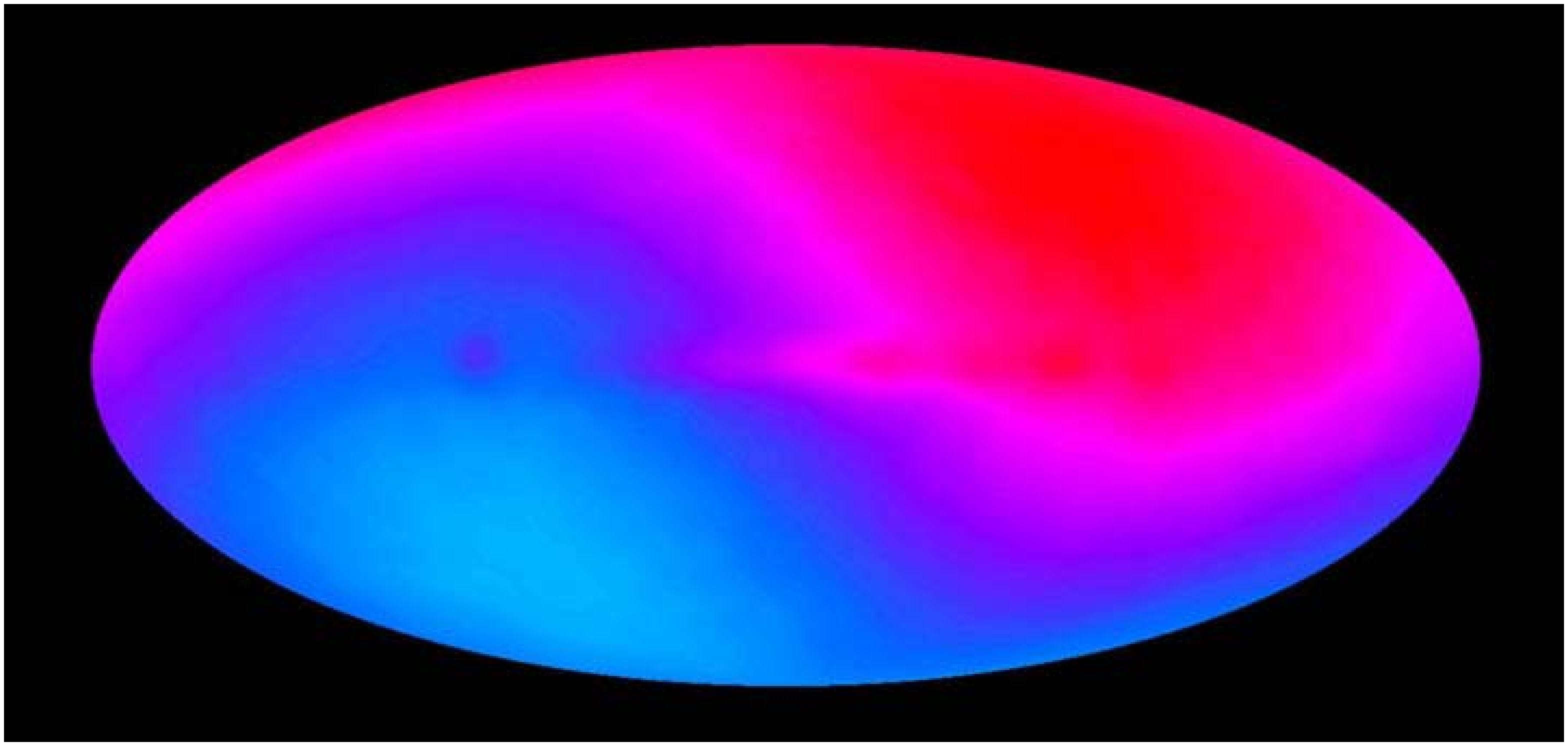

Our velocity through the CMB: 390 km/sec

Doppler effect produces spatial variation in CMB temperature: 2.73K + 0.1% and – 0.1%

COBE differential microwave radiometer

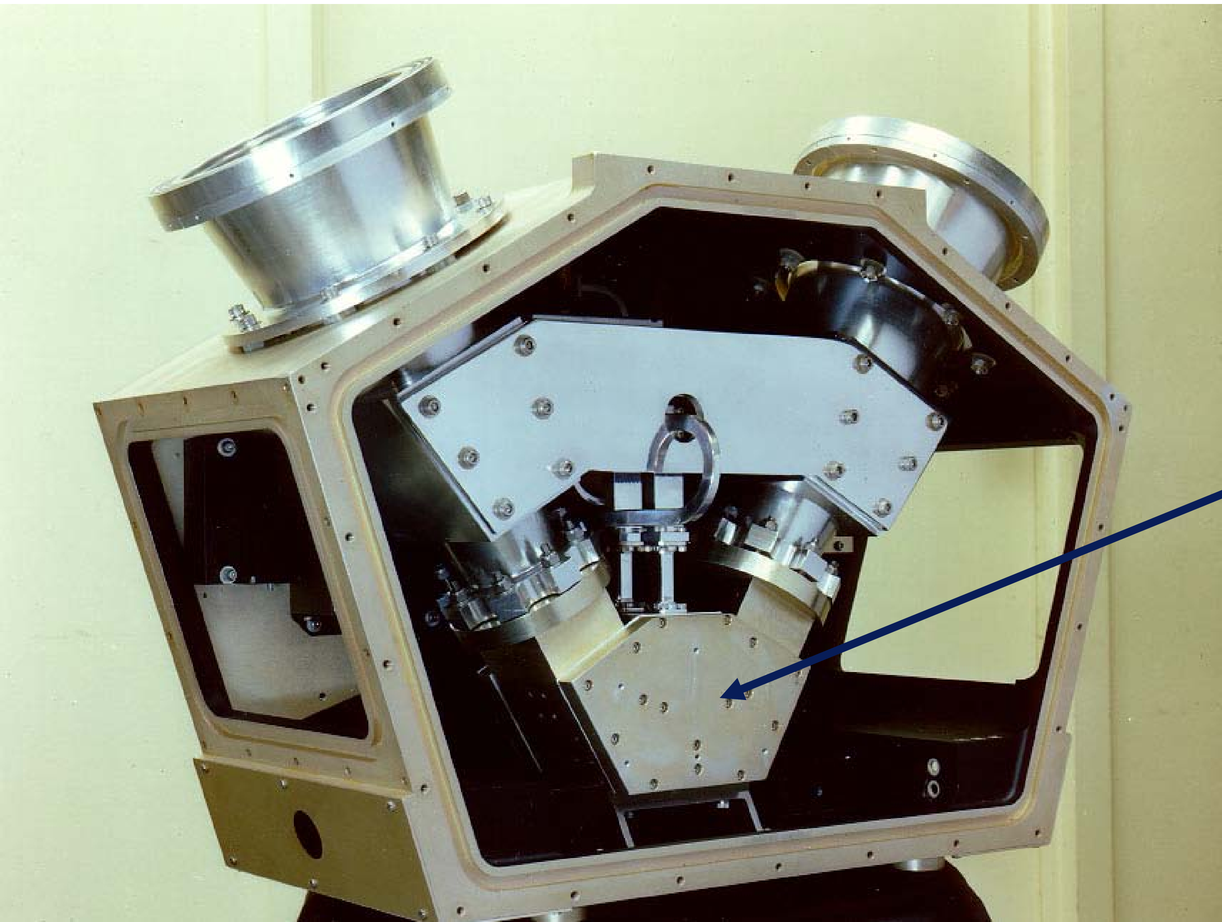

Dicke switch

COBE systematic errors

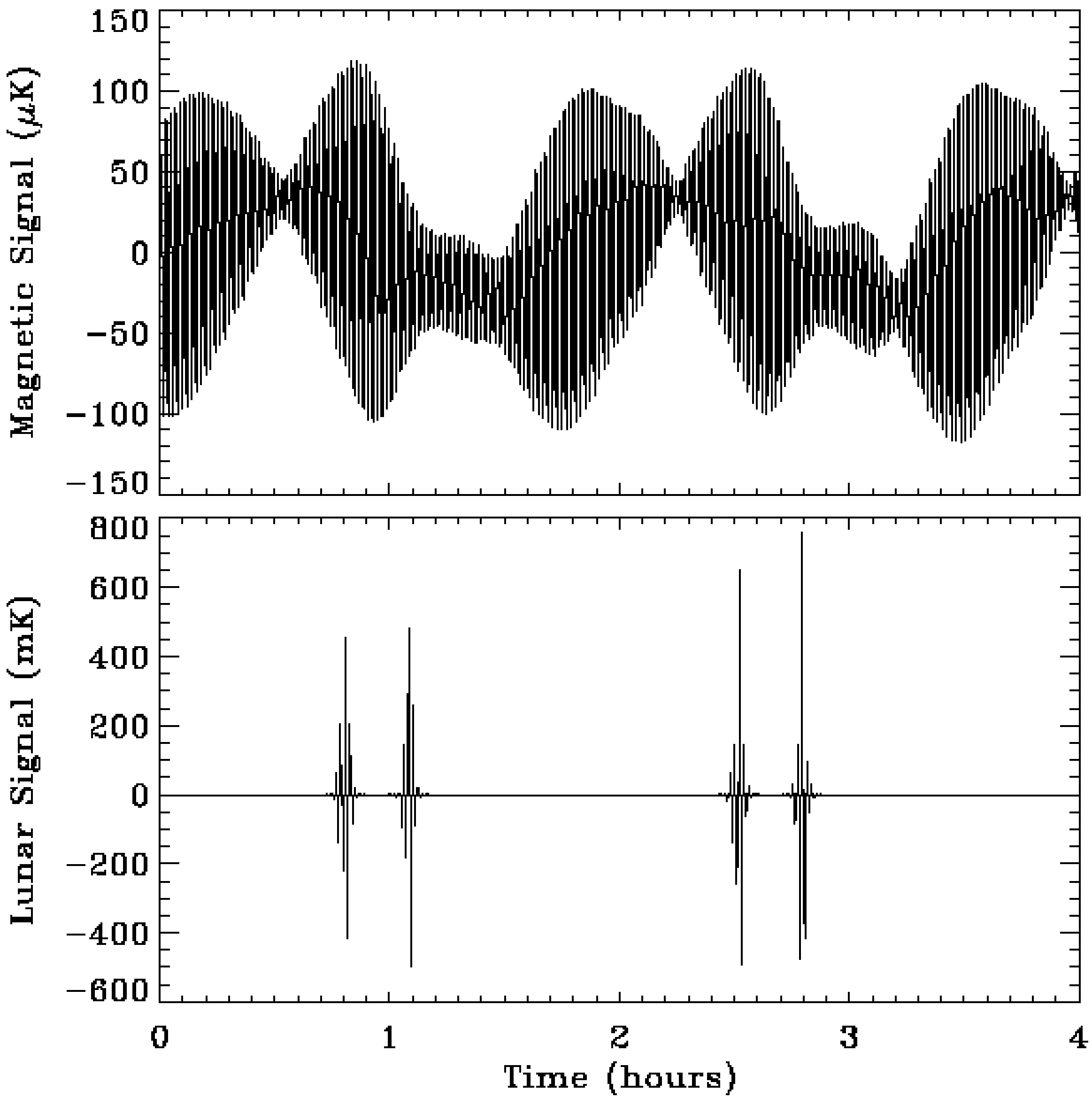

The largest systematic error was the Earth's magnetic field coupling into the 100 Hz magnetically switched ferrite circulator in the Dicke switch, creating time-varying extra insertion loss. This figure shows the COBE magnetic and celestial signals vs time for 53B channel.

(top) Magnetic signal from the Earth's field. The spin and orbit modulation are clearly apparent. Note that this systematic is ten times larger than the dipole-subtracted anisotropy signal!

(bottom) Celestial signal from an unresolved source (the Moon).

The COBE team had to model and subtract these systematics after the mission. Residual systematic error resulted from model and fitting errors.

WMAP

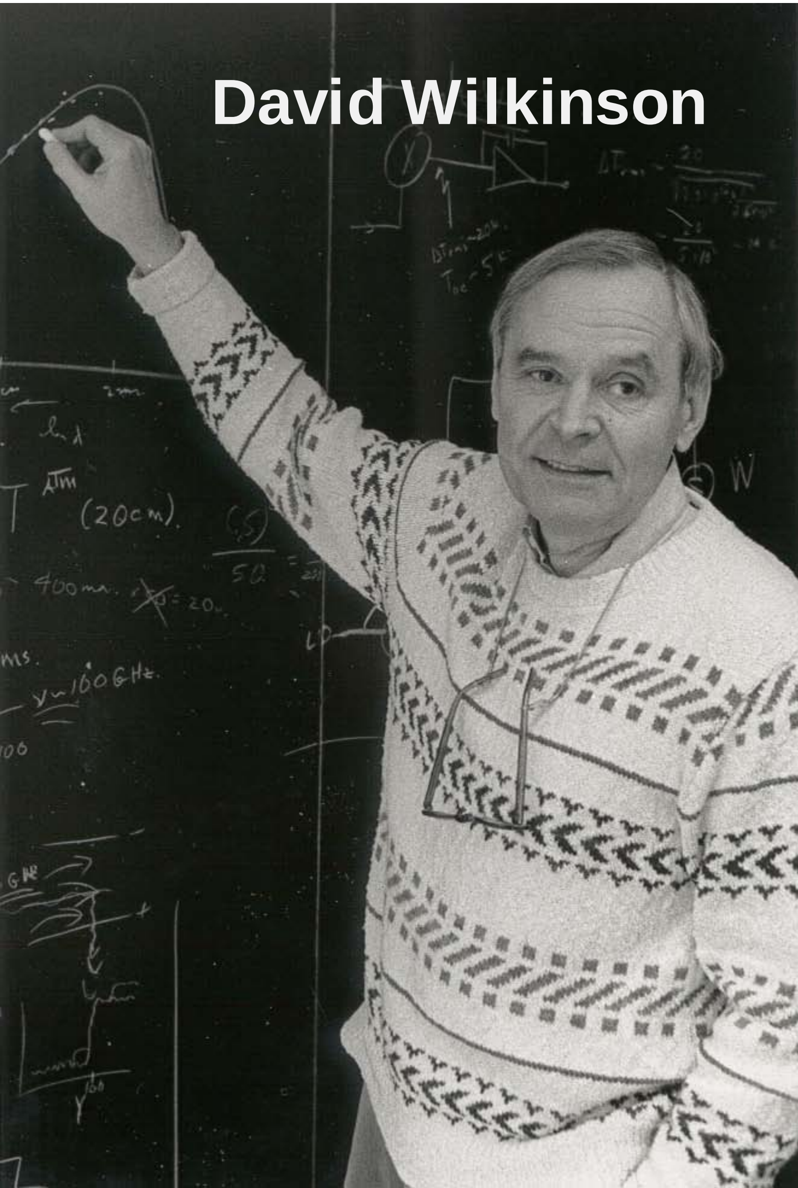

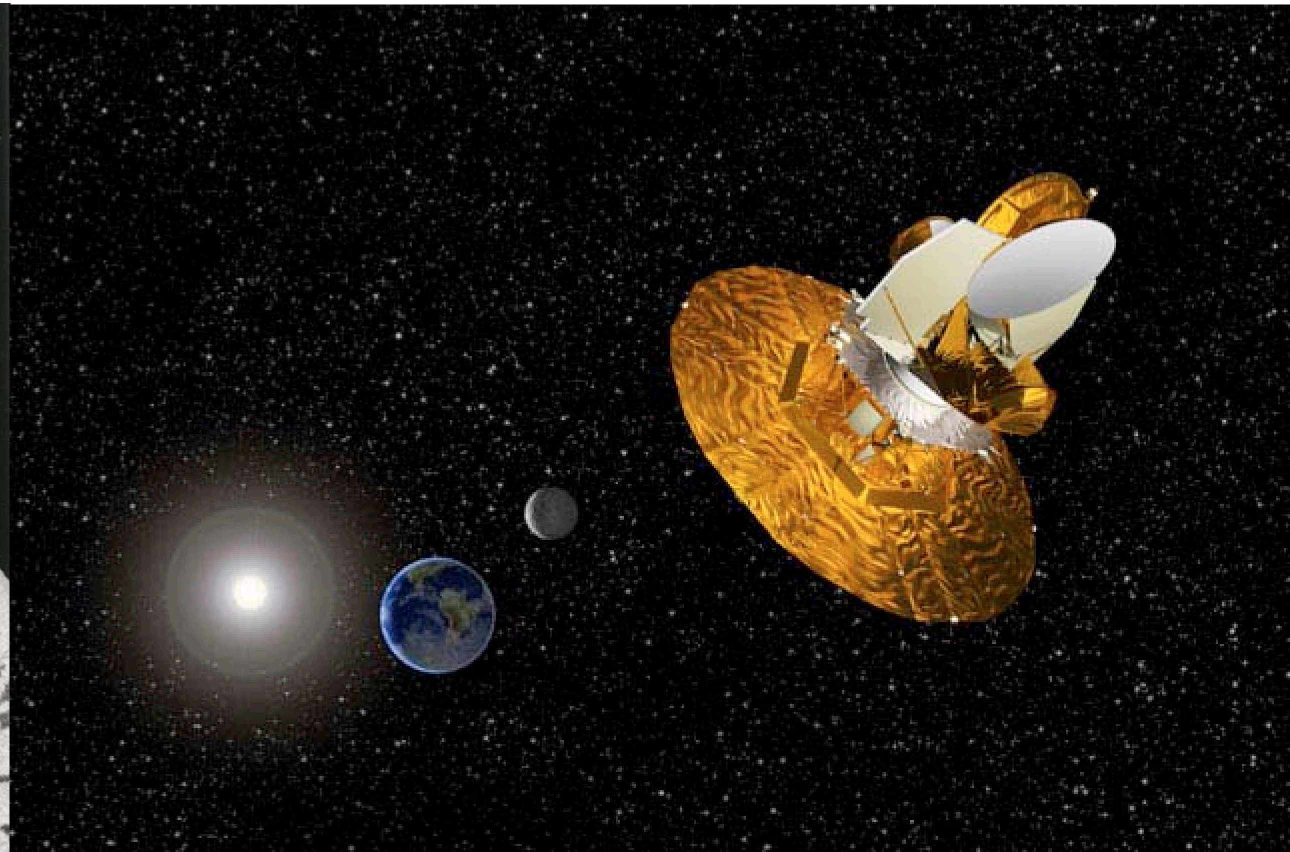

WMAP

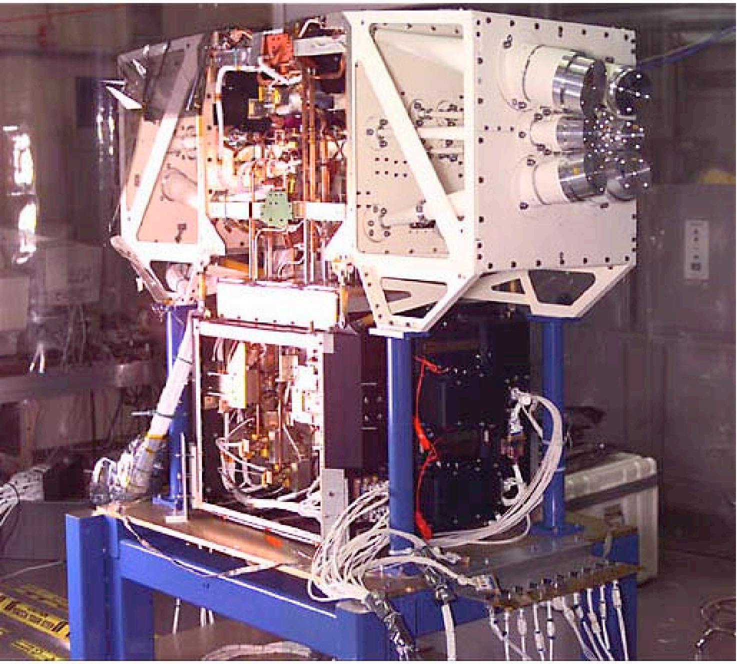

MAP990259

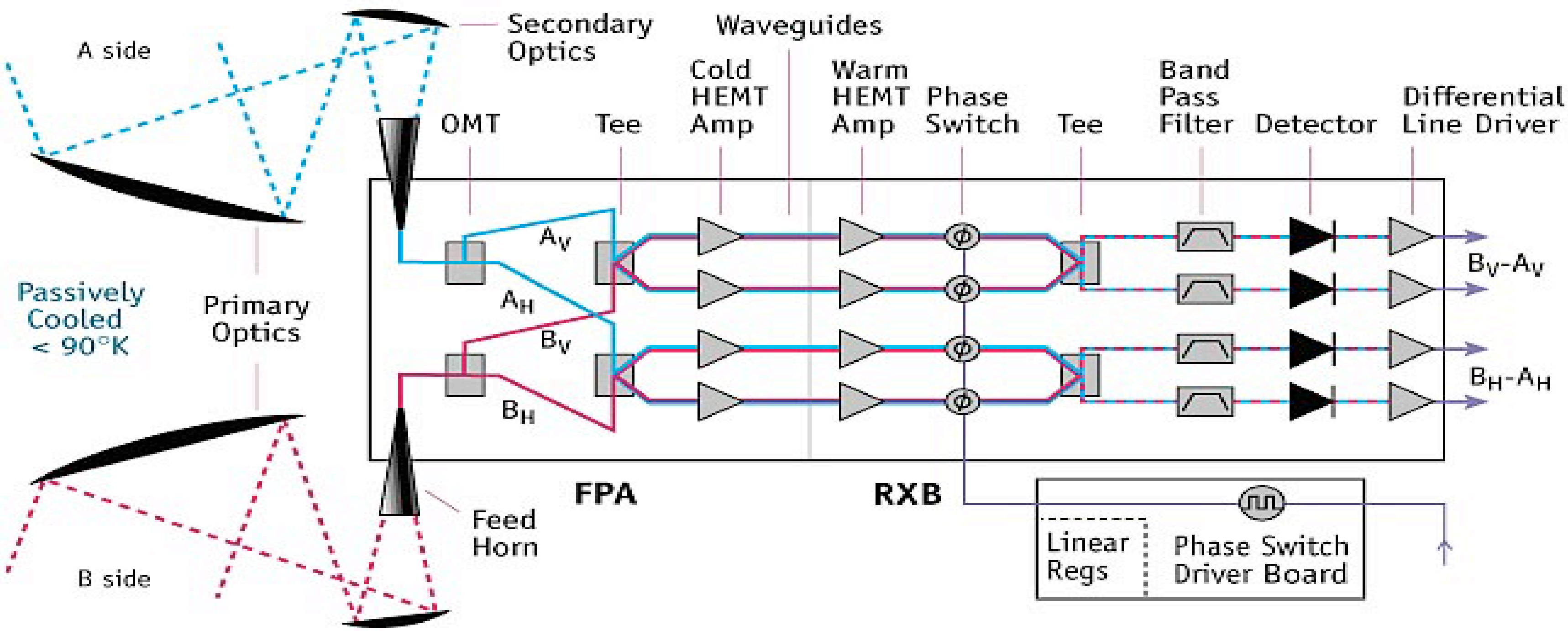

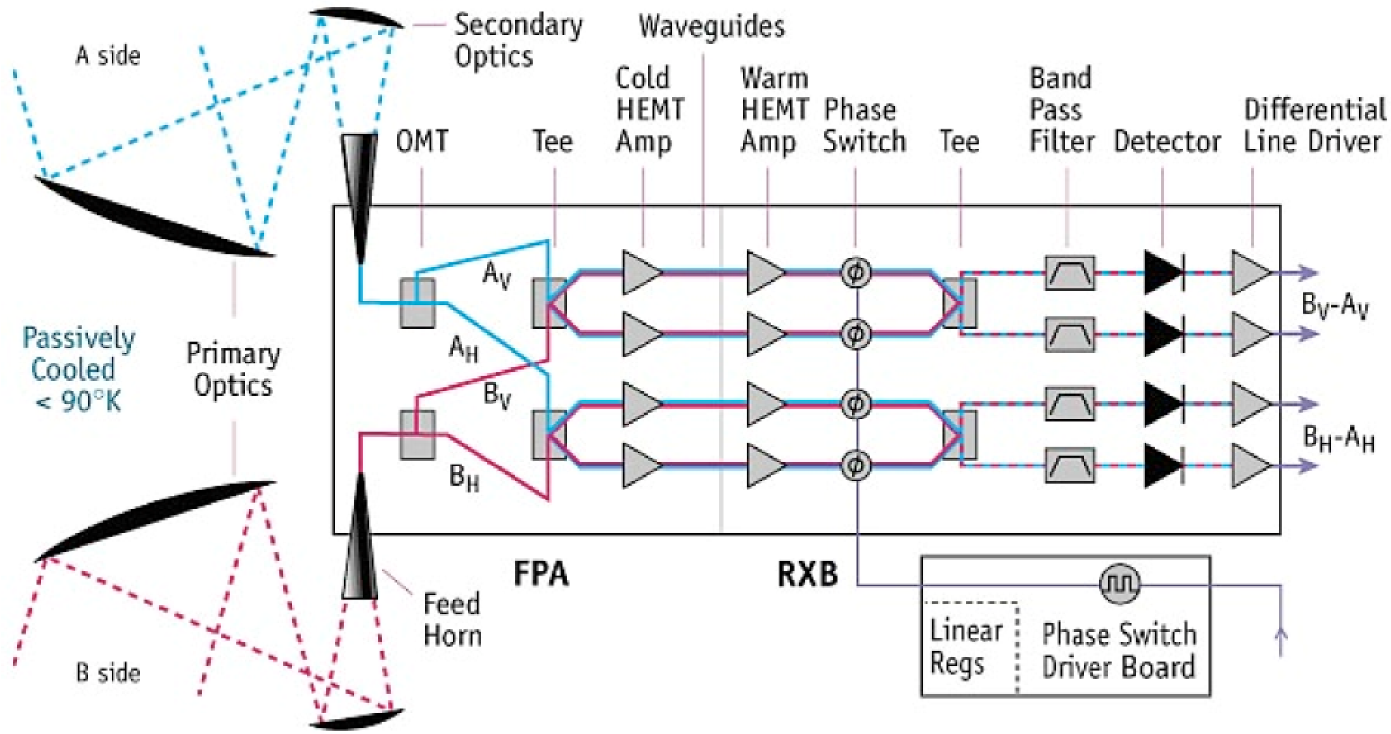

WMAP receiver “Dicke” switching scheme

Since the signals to be differenced are amplified by both amplifier chains, gain fluctuations in either amplifier chain act identically on both signals and thus cancel upon differencing.
The phase switches introduce a 180 degree relative phase change between the two signal paths, thereby interchanging which signal is fed to which square law detector. Thus, low frequency noise from the detector diodes is common mode and also cancels, further reducing susceptibility to systematic effects.

MAP990202

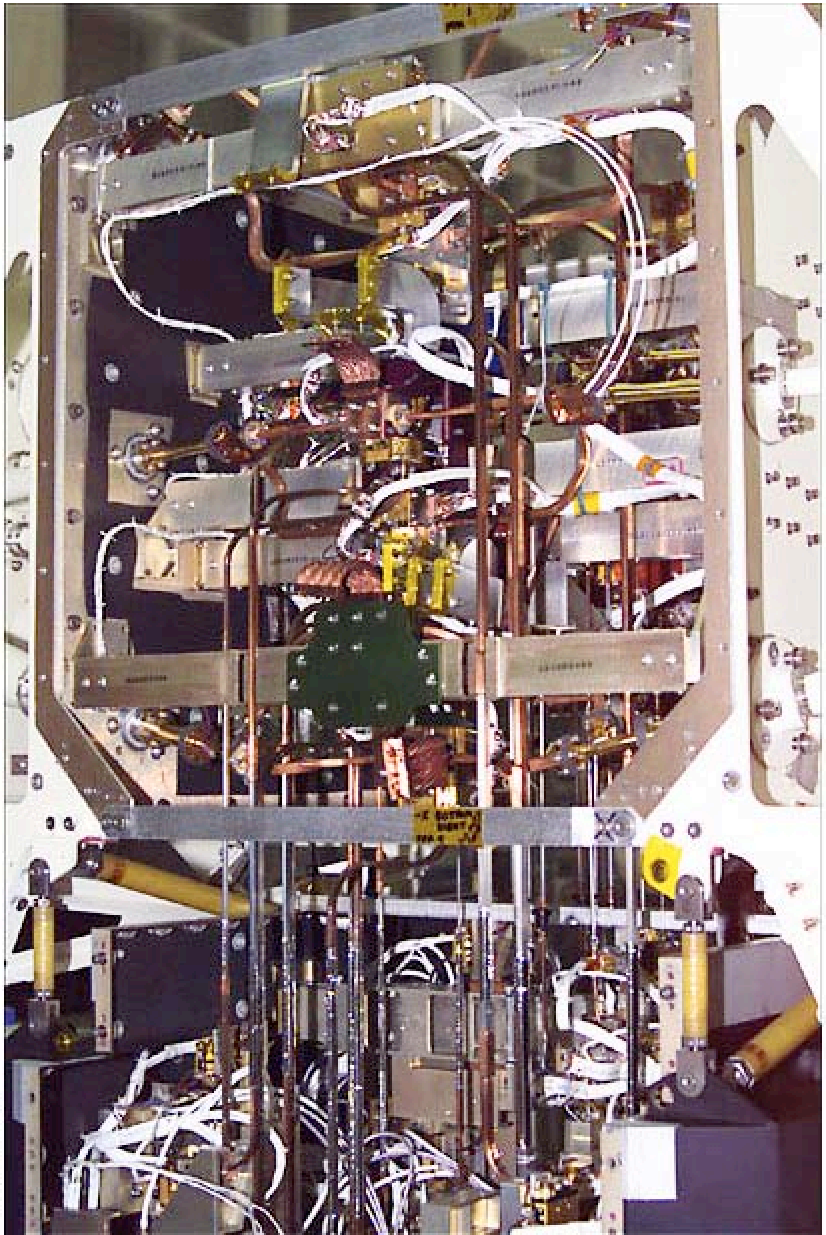

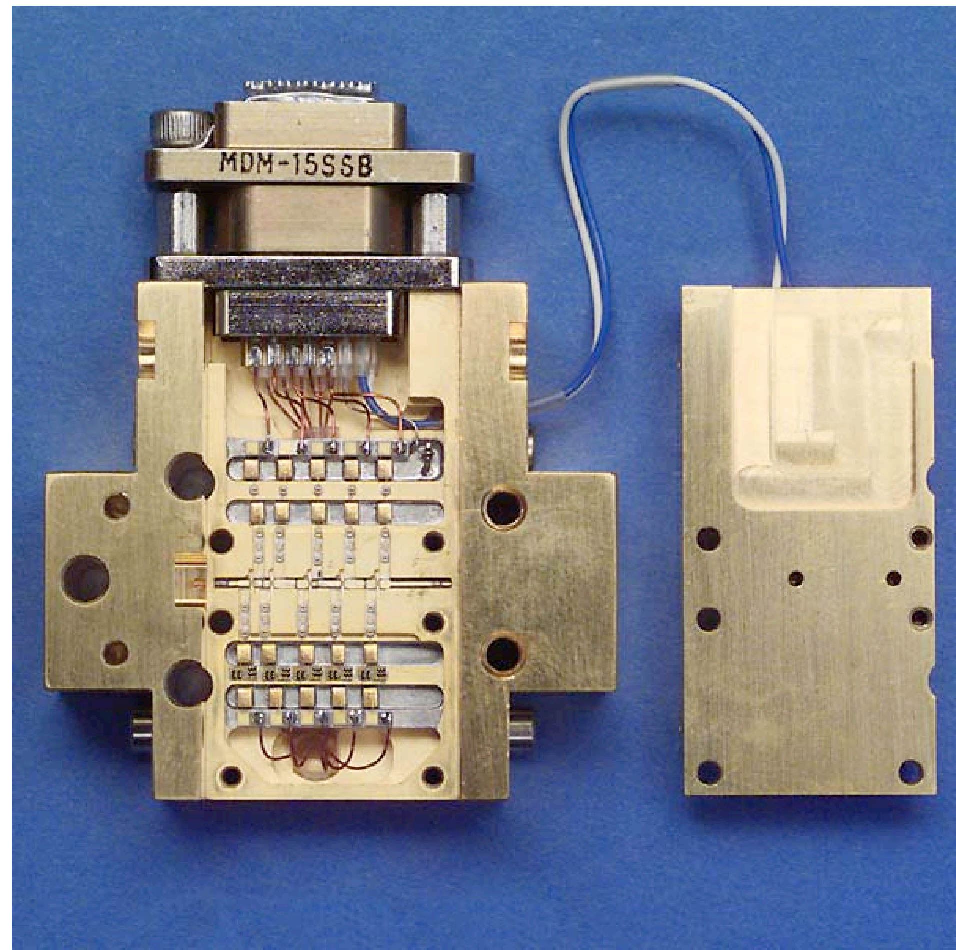

CMB Temperature smooth to 3 Decimal places

CMB "dipole" (at the 0.1% level)

Interpret CMB dipole as red/blue shifts due to our motion and remove to get "cosmic anisotropies"

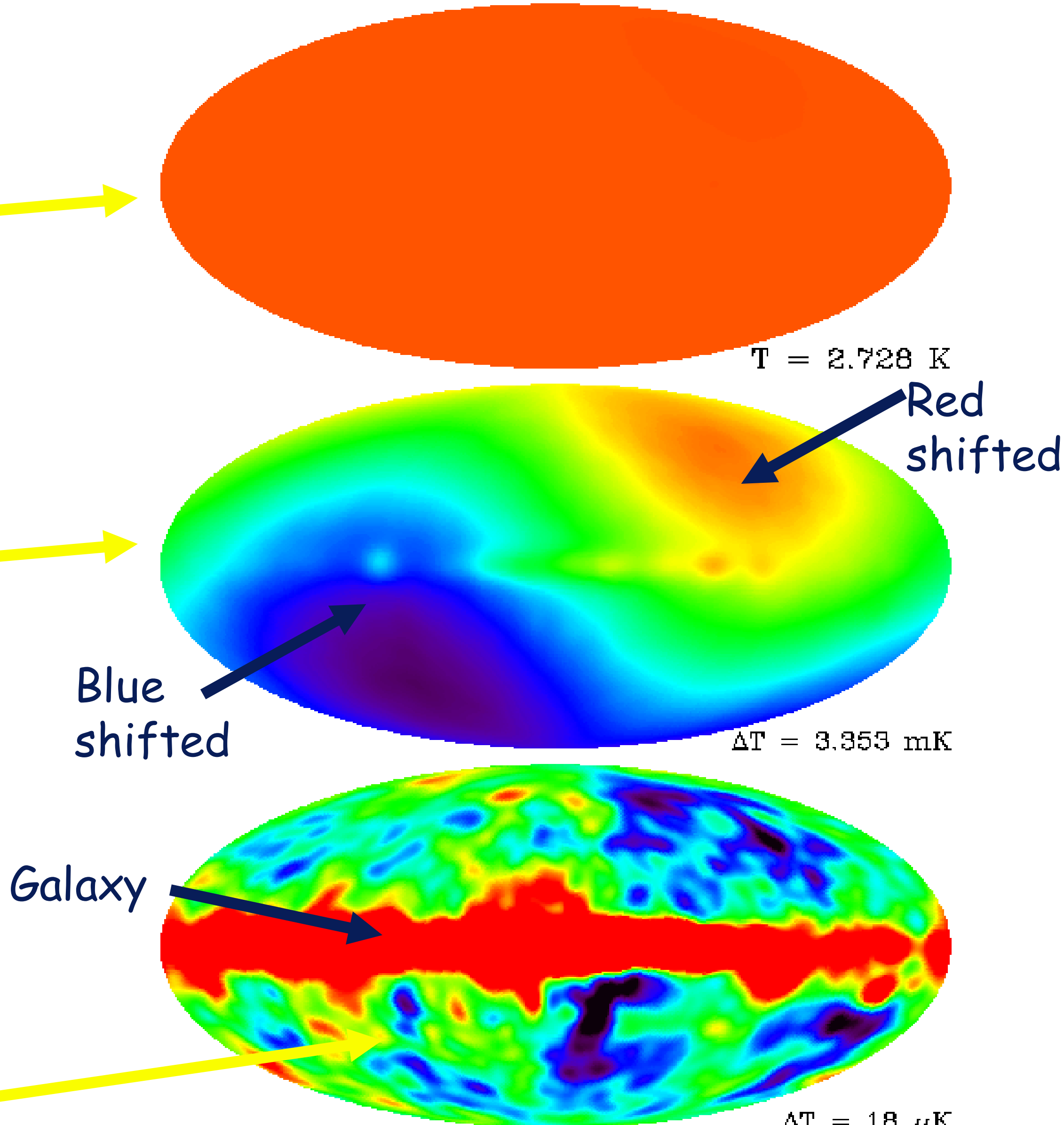

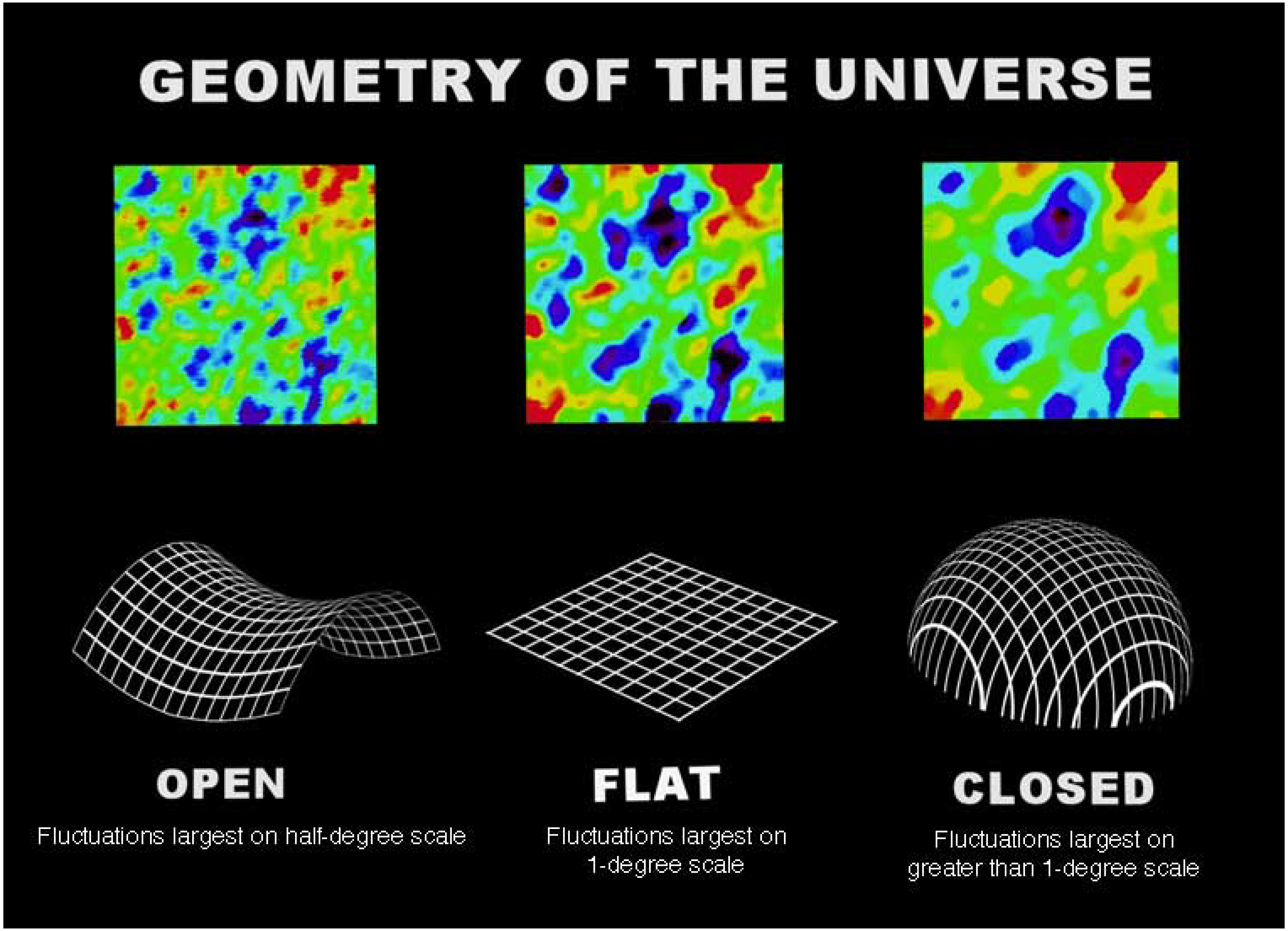
GEOMETRY OF THE UNIVERSE
OPEN
Fluctuations largest on half-degree scale
FLAT
Fluctuations largest on 1-degree scale
CLOSED
Fluctuations largest on greater than 1-degree scale

five frequency maps

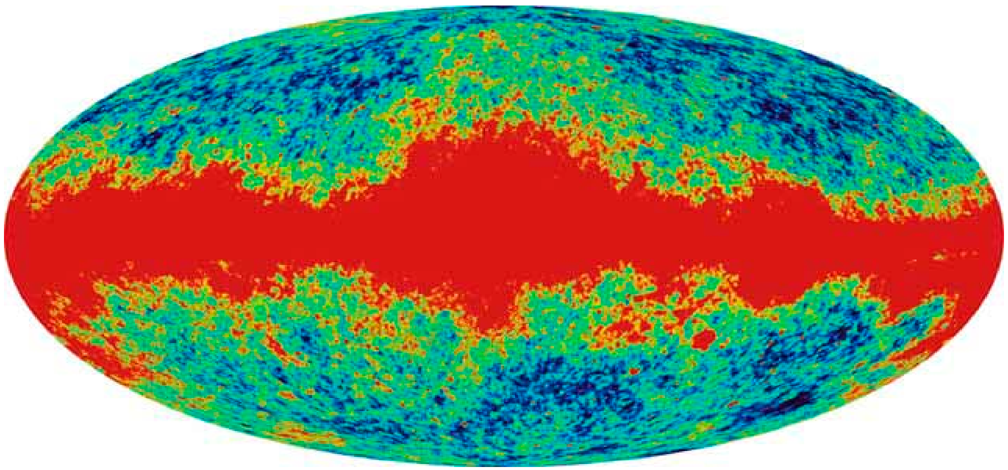

23, 33, 41, 61 and 93 GHz

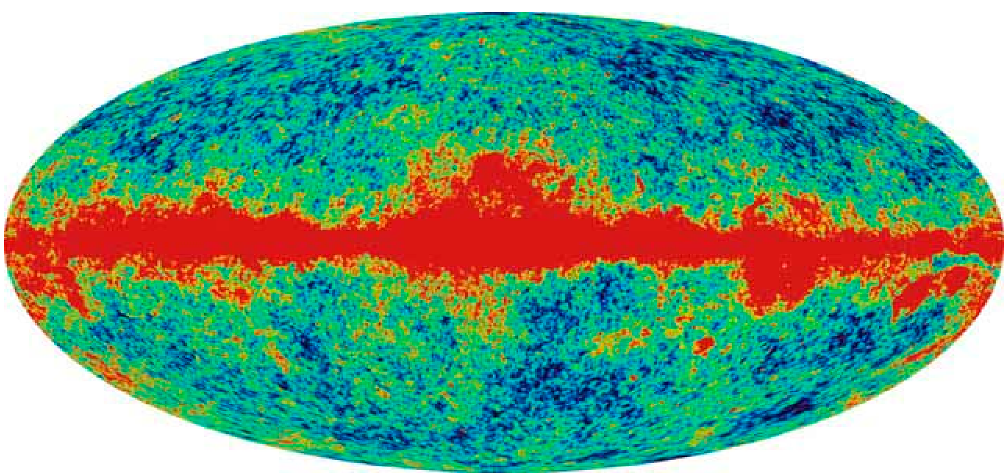

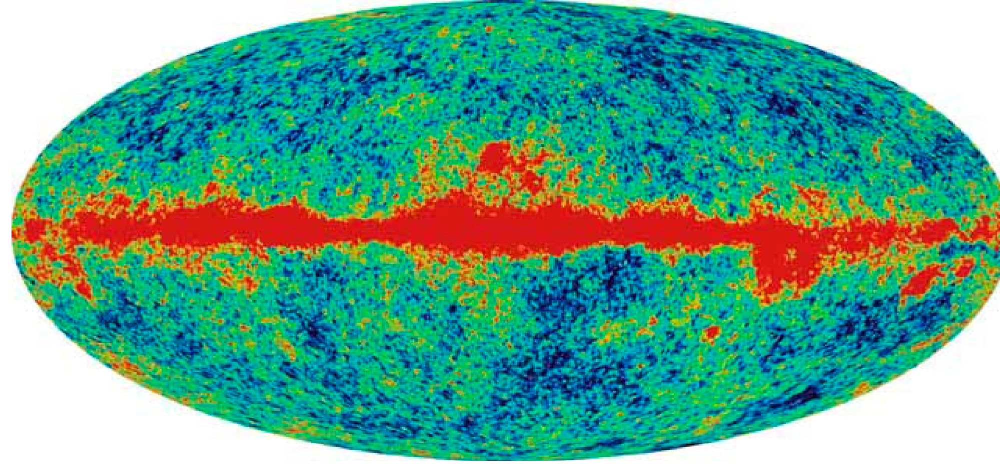

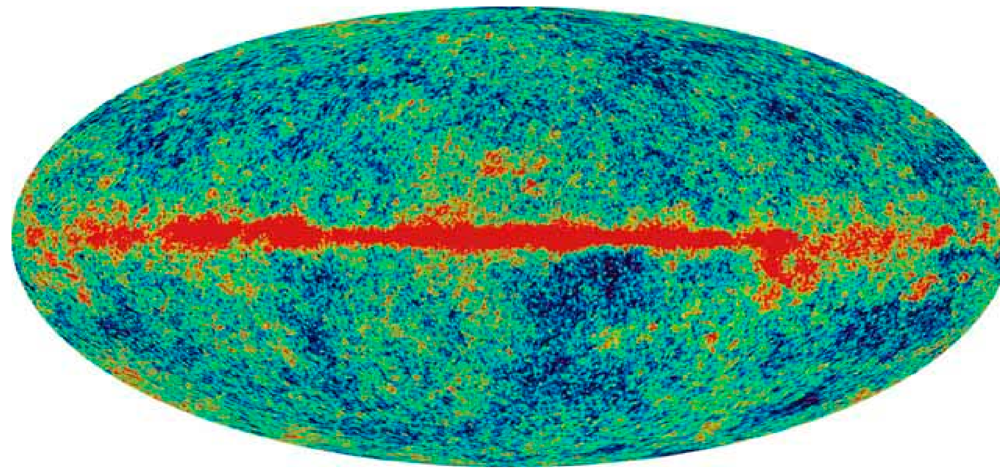

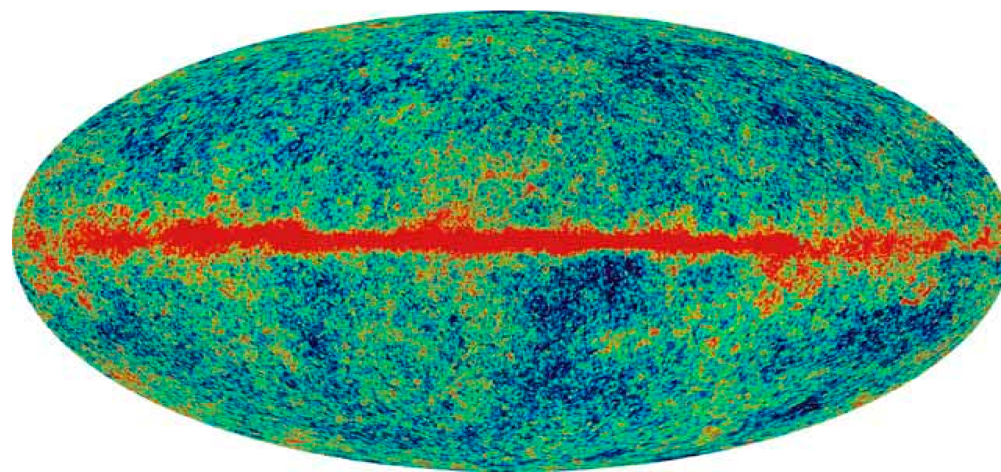

derived maps

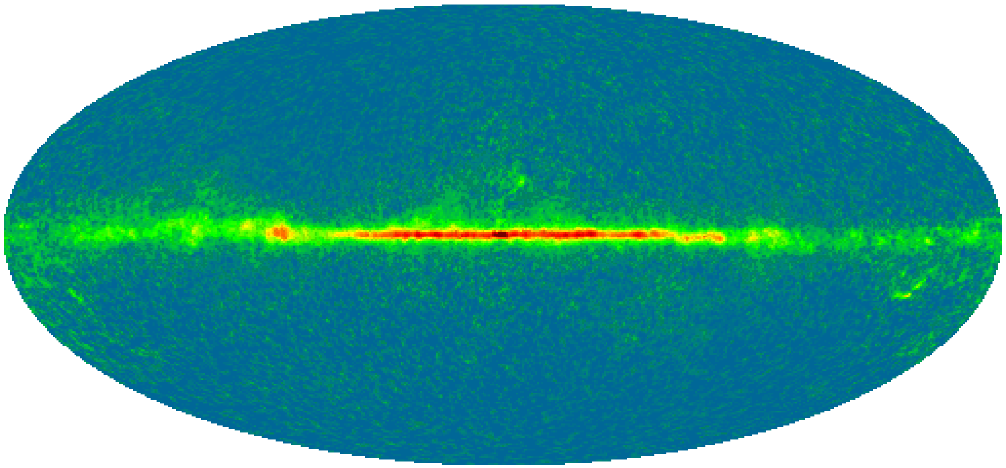

Dust map

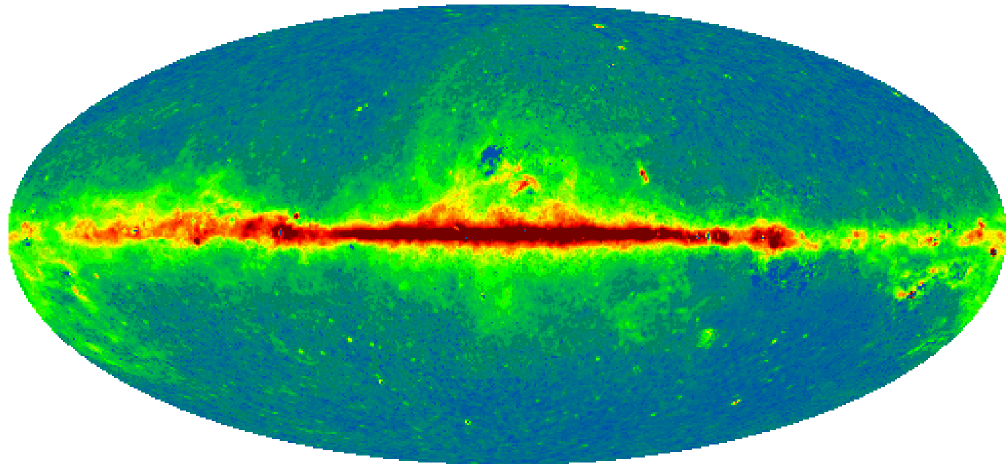

Synchrotron map

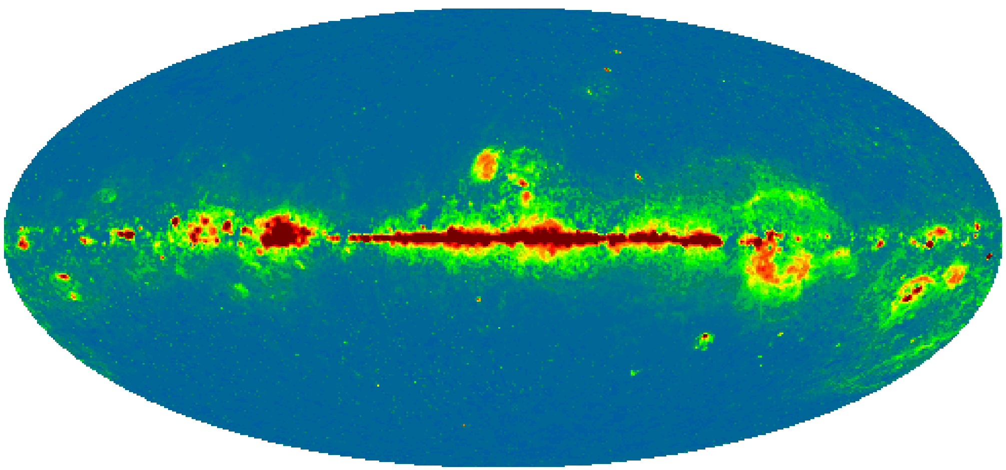

Free-free map

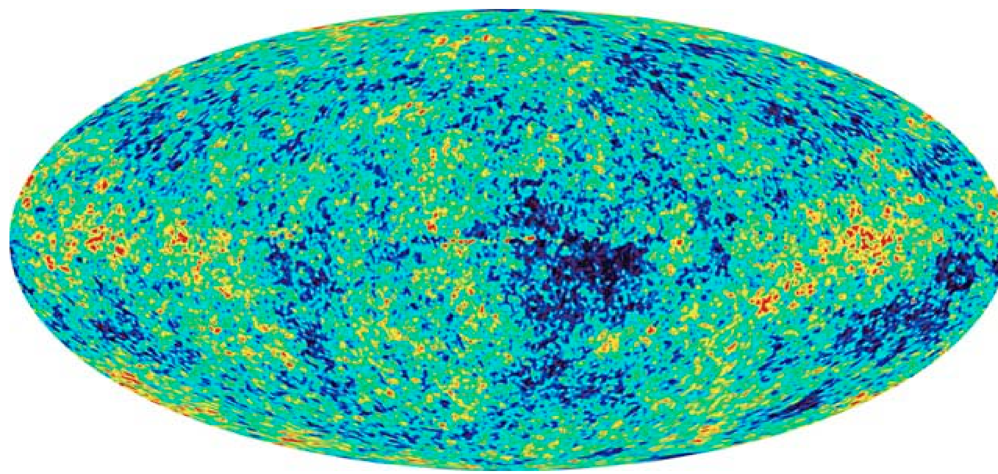

CMB map

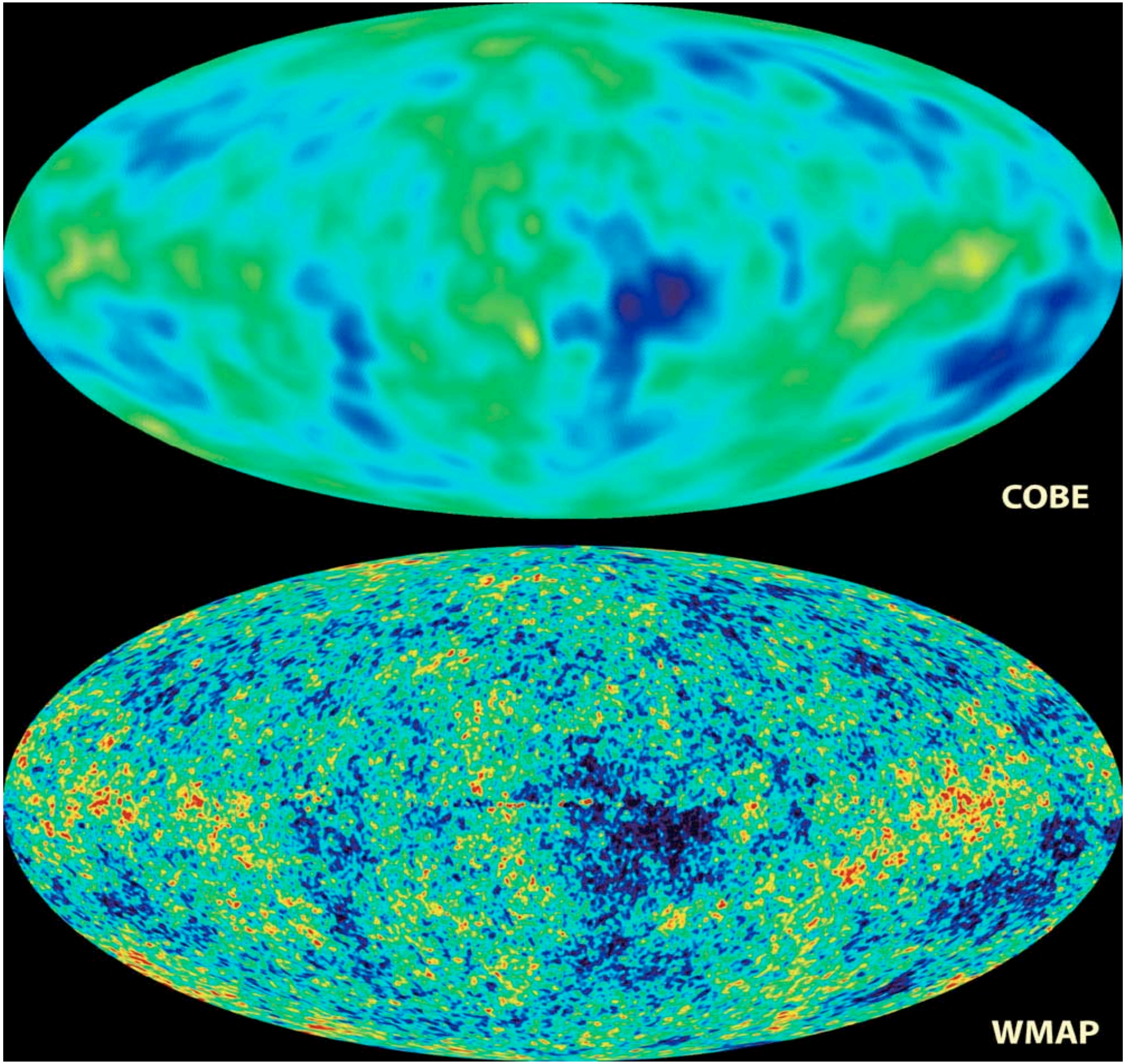
COBE
WMAP

WMAP CMB power spectrum

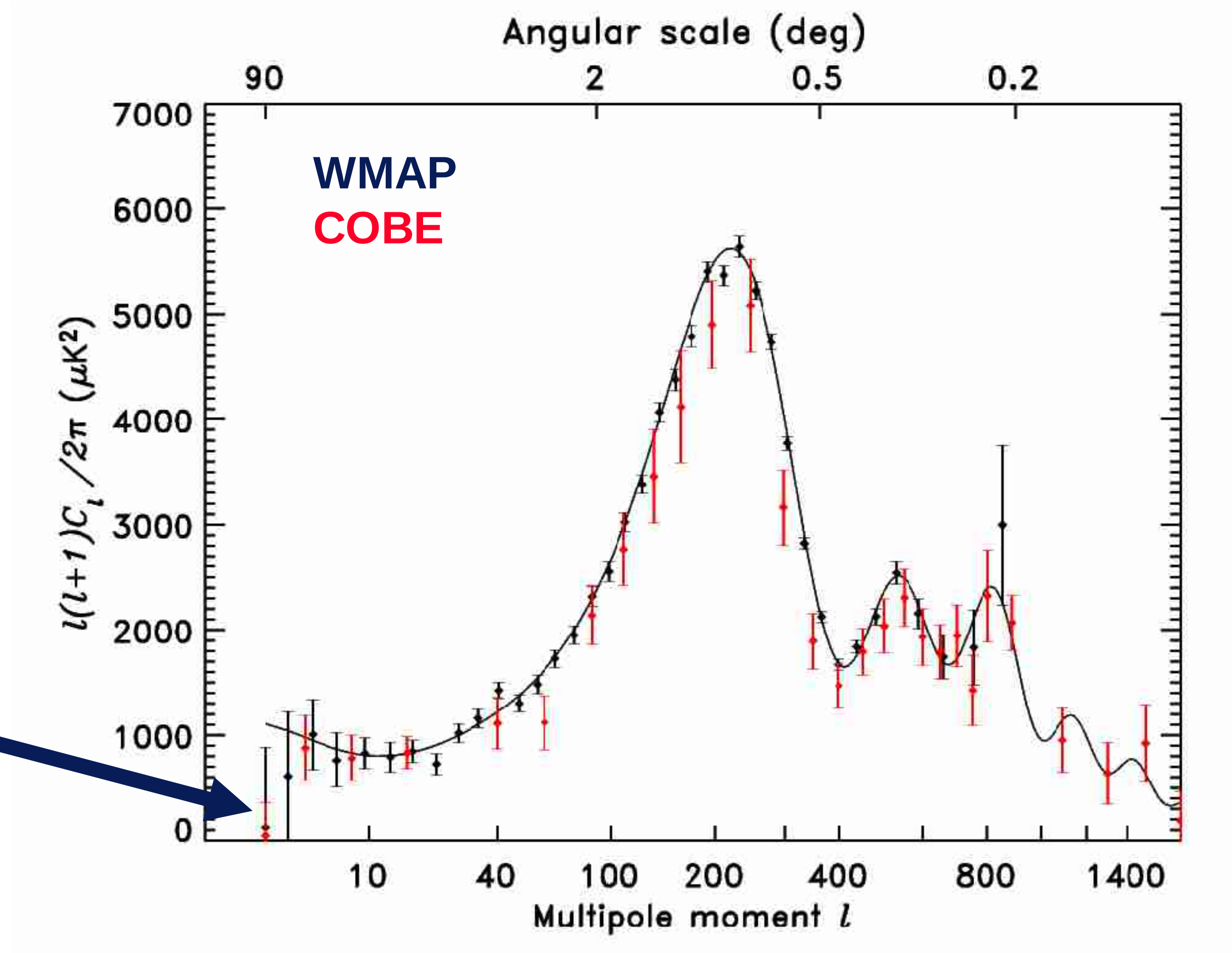

Note deficit of power on large angular scales, observed first by COBE and confirmed by WMAP. Common systematic error or hint of new physics?

Systematic error?

The large-angle correlations of the Cosmic Microwave Background exhibit several statistically significant anomalies compared to the standard inflationary big-bang model. This finding casts doubts on the cosmological interpretation of the lowest multipoles from the temperature-temperature correlation and from the temperature-polarization correlation.

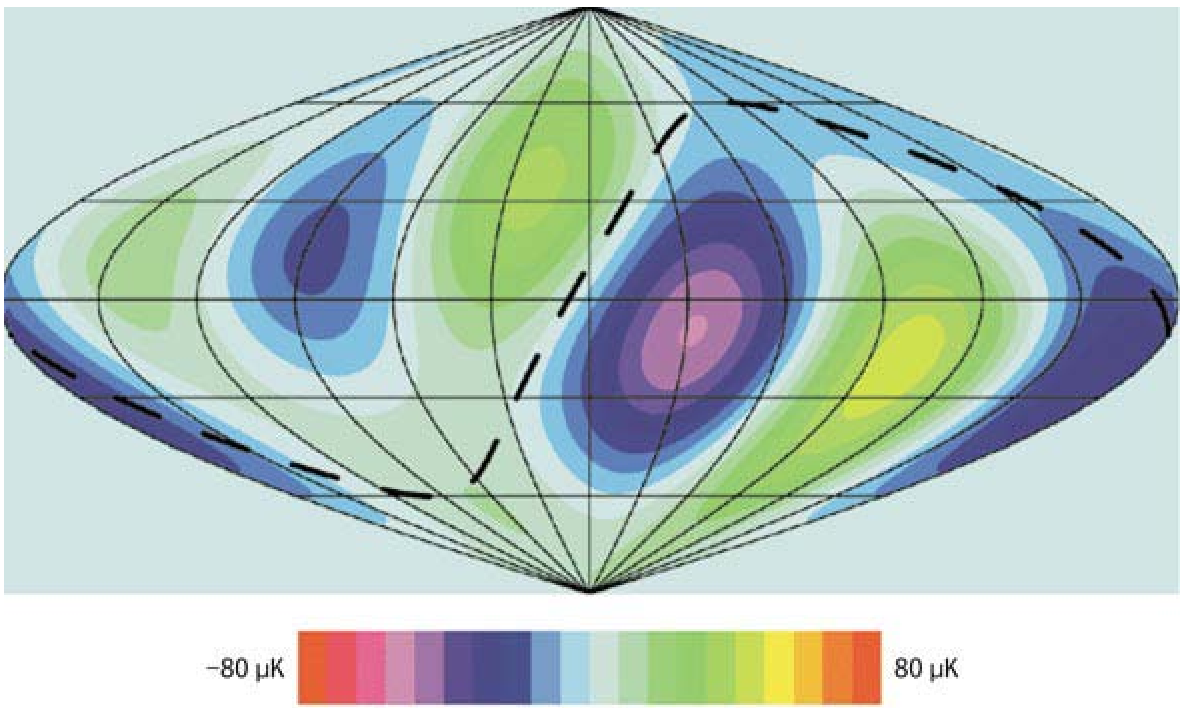

Pictured here is a combined quadrupole plus octopole map of the WMAP microwave sky in galactic co-ordinates, after subtracting the Milky Way. The ecliptic (dashed line) threads its way along the node line, separating one of the hot spots from one of the cold spots, tracking the node over a third of the sky.

WMAP scan strategy

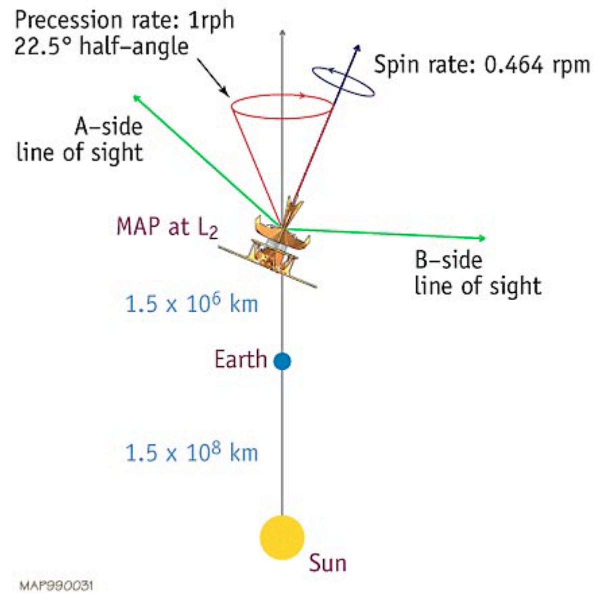

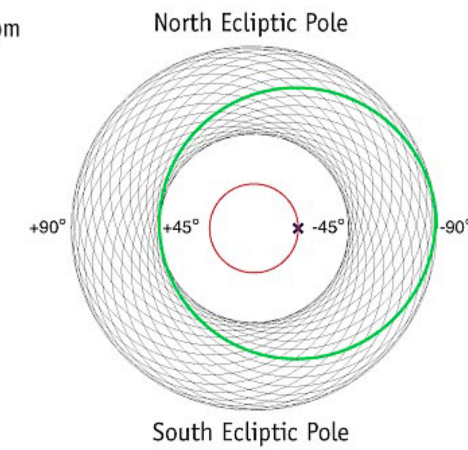

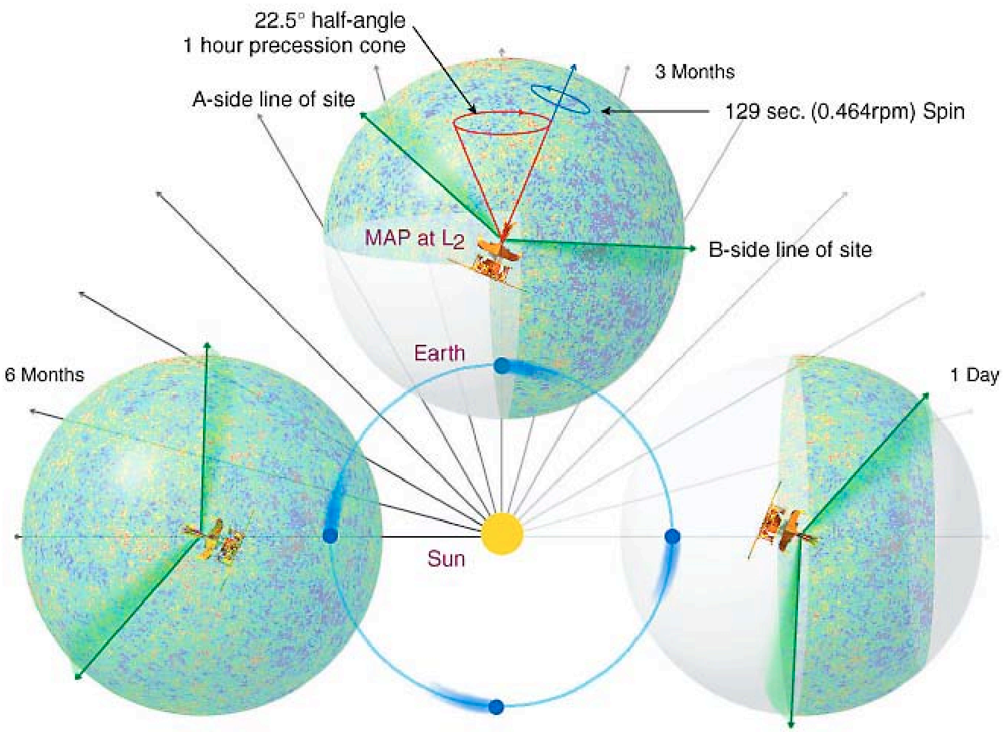

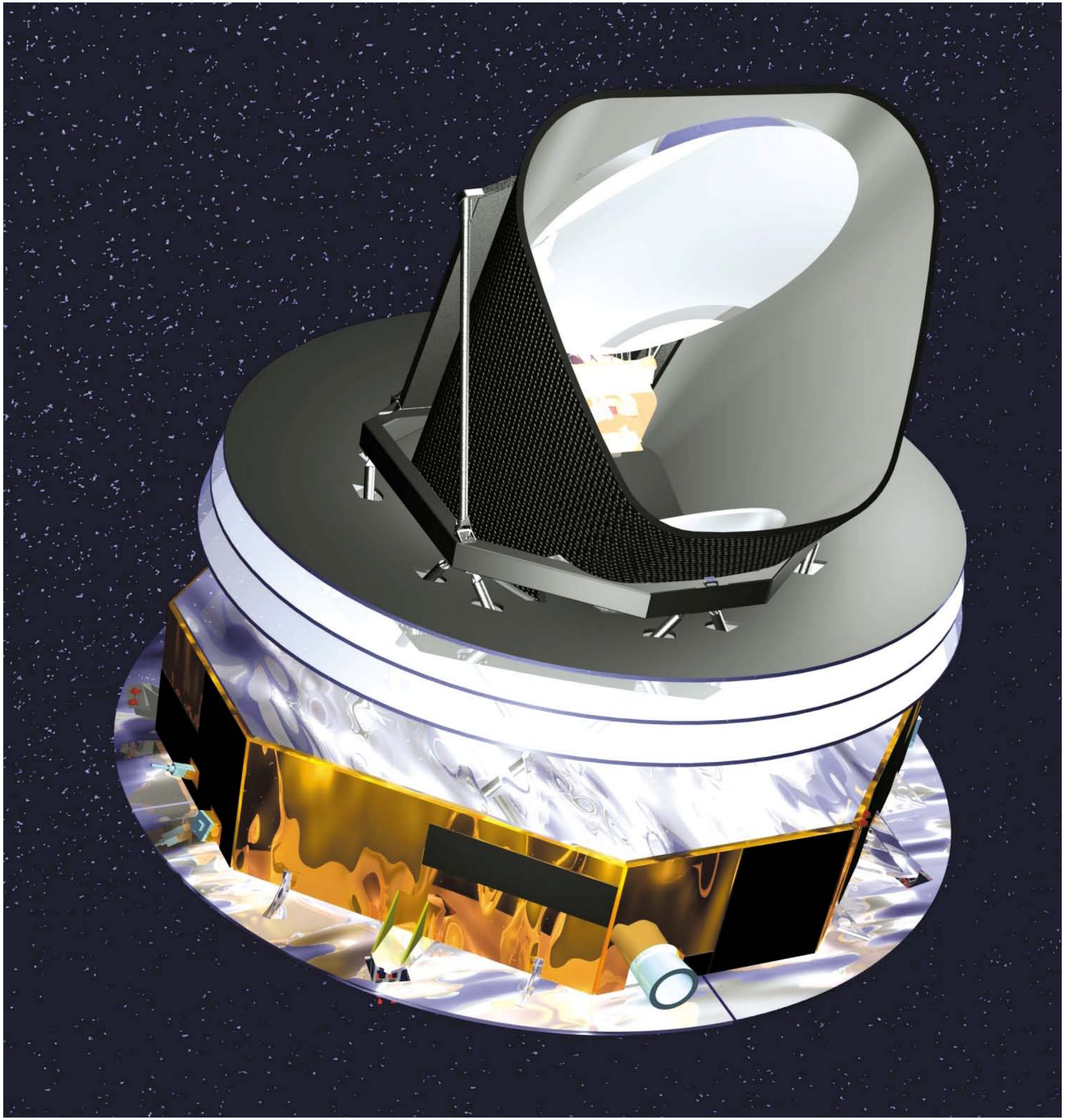

Planck focal plane (Low Freq Instrument)

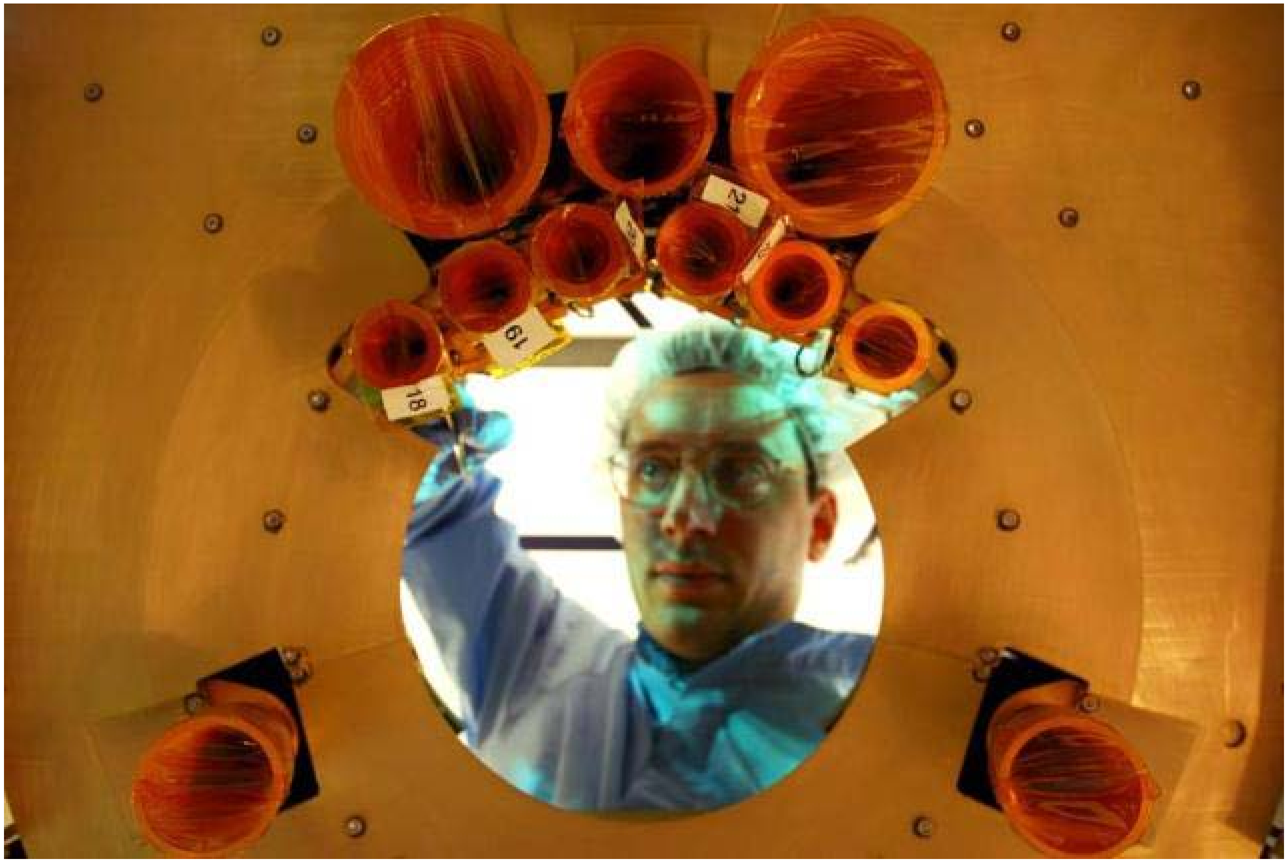

Planck on its way

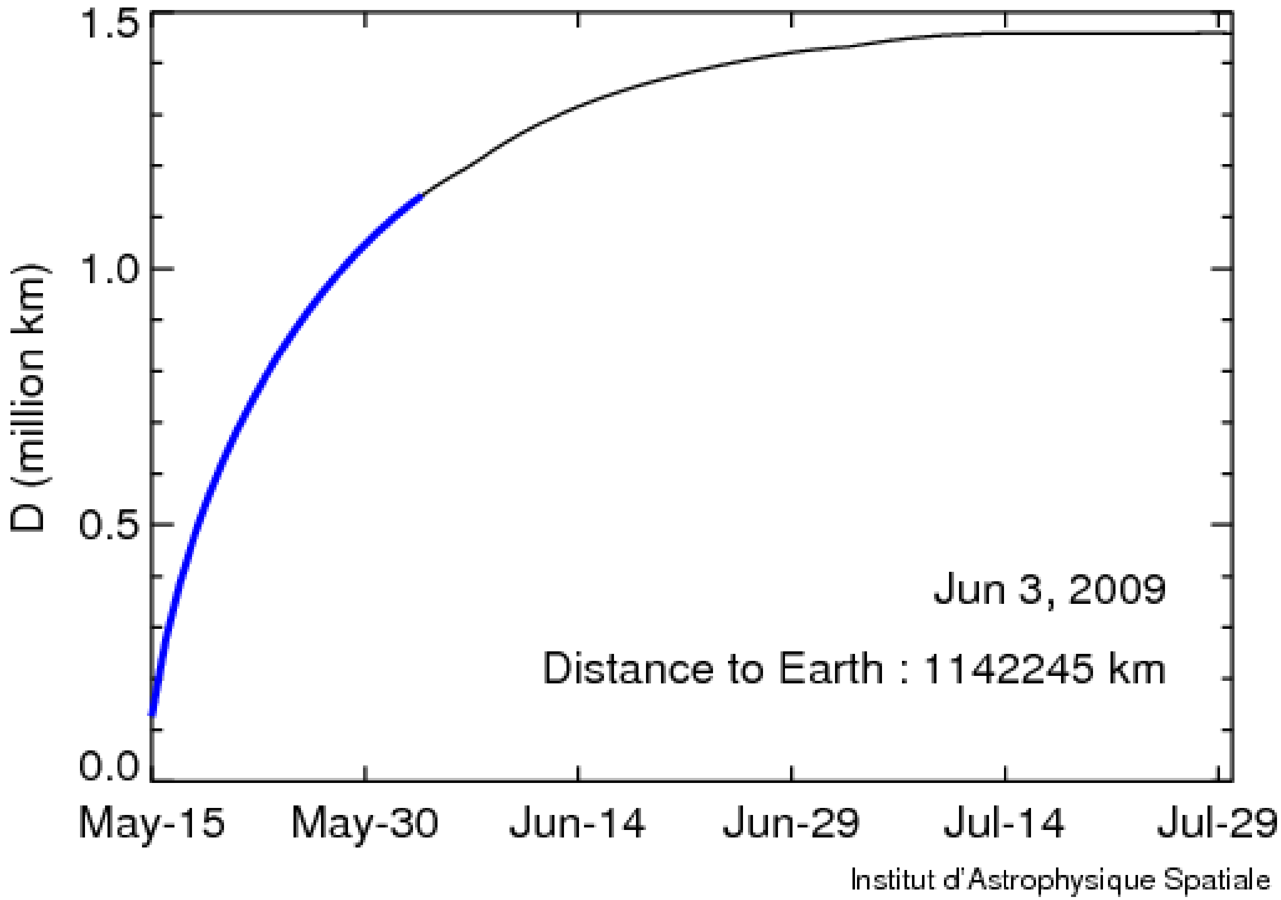

Planck scan

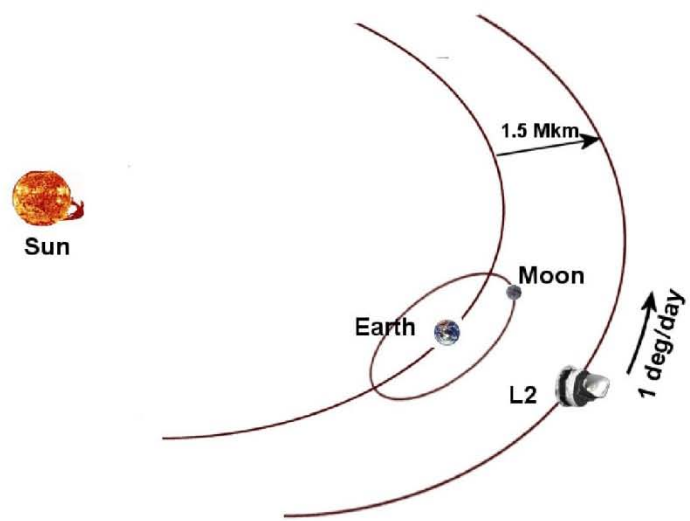

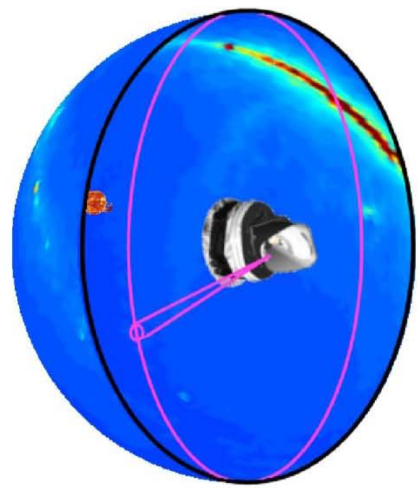

Comparison with WMAP

WMAP

- **22-90 GHz**
- **13’**
- **300 uK-arcmin (@ 94 GHz)**
- **420 uK-arcmin (polarization @ 94 GHz)**

Planck

- **30-850 GHz**
- **5’ (@>=217 GHz)**
- **40 uK-arcmin (@143 GHz)**
- **80 uK-arcmin (polarization @143 GHz)**

Temperature Maps

Planck Bluebook

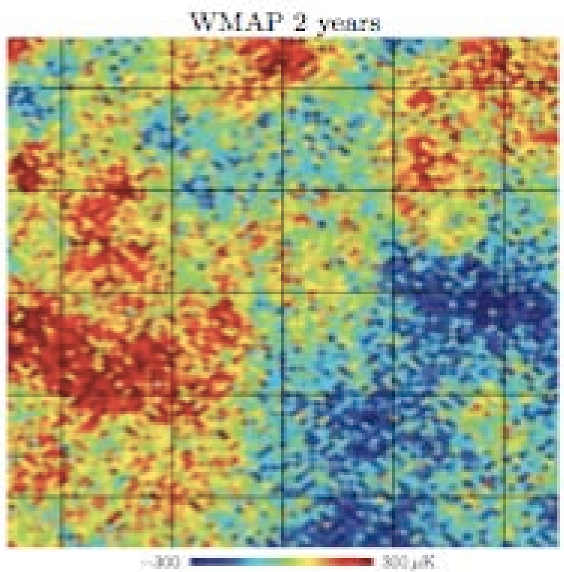

WMAP 2 years

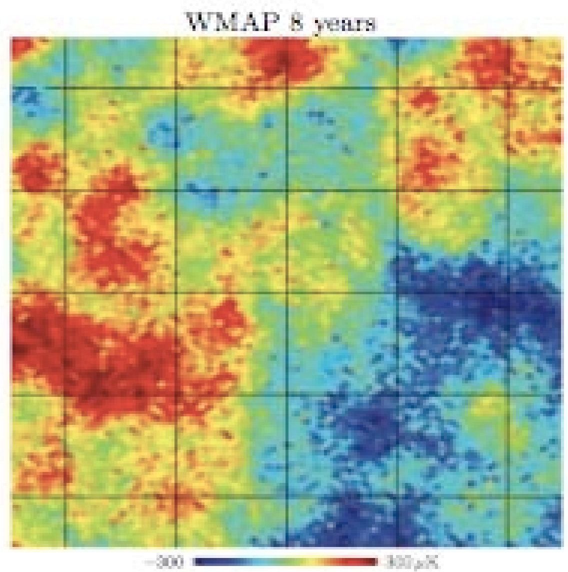

WMAP 8 years

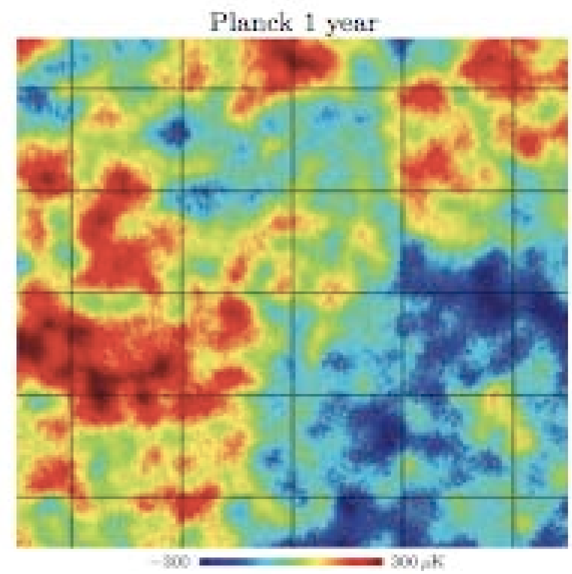

Planck 1 year

Planck Bluebook

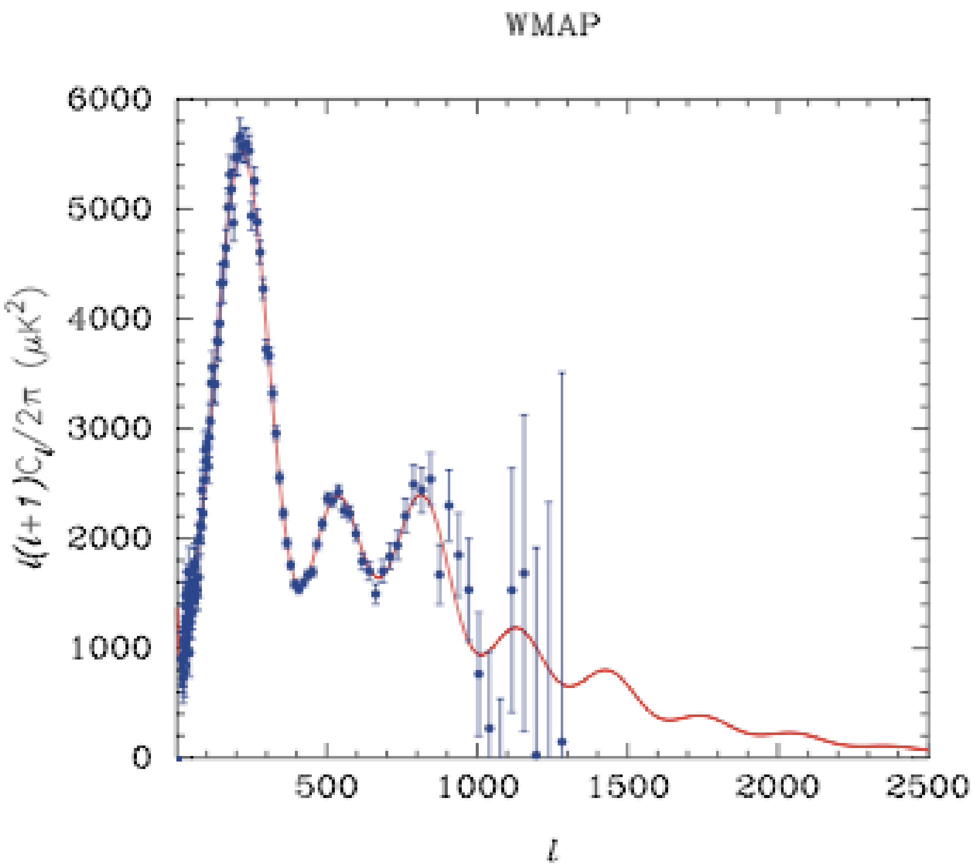

WMAP 4 years

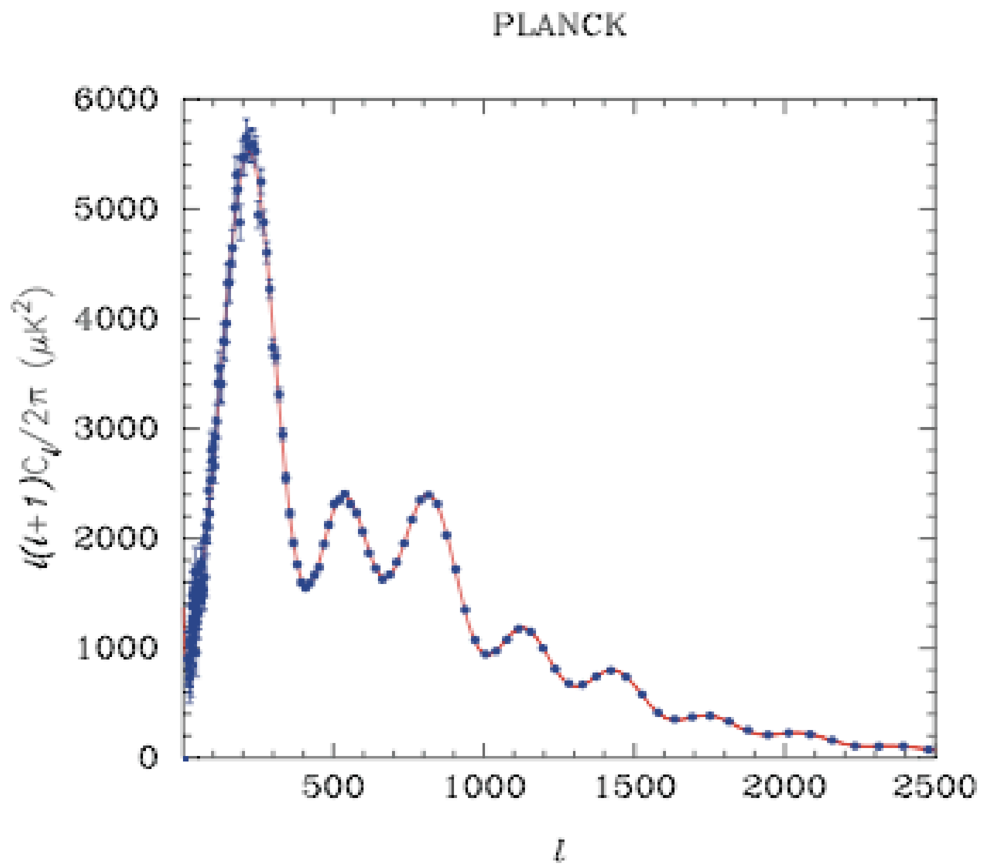

Planck 1 year

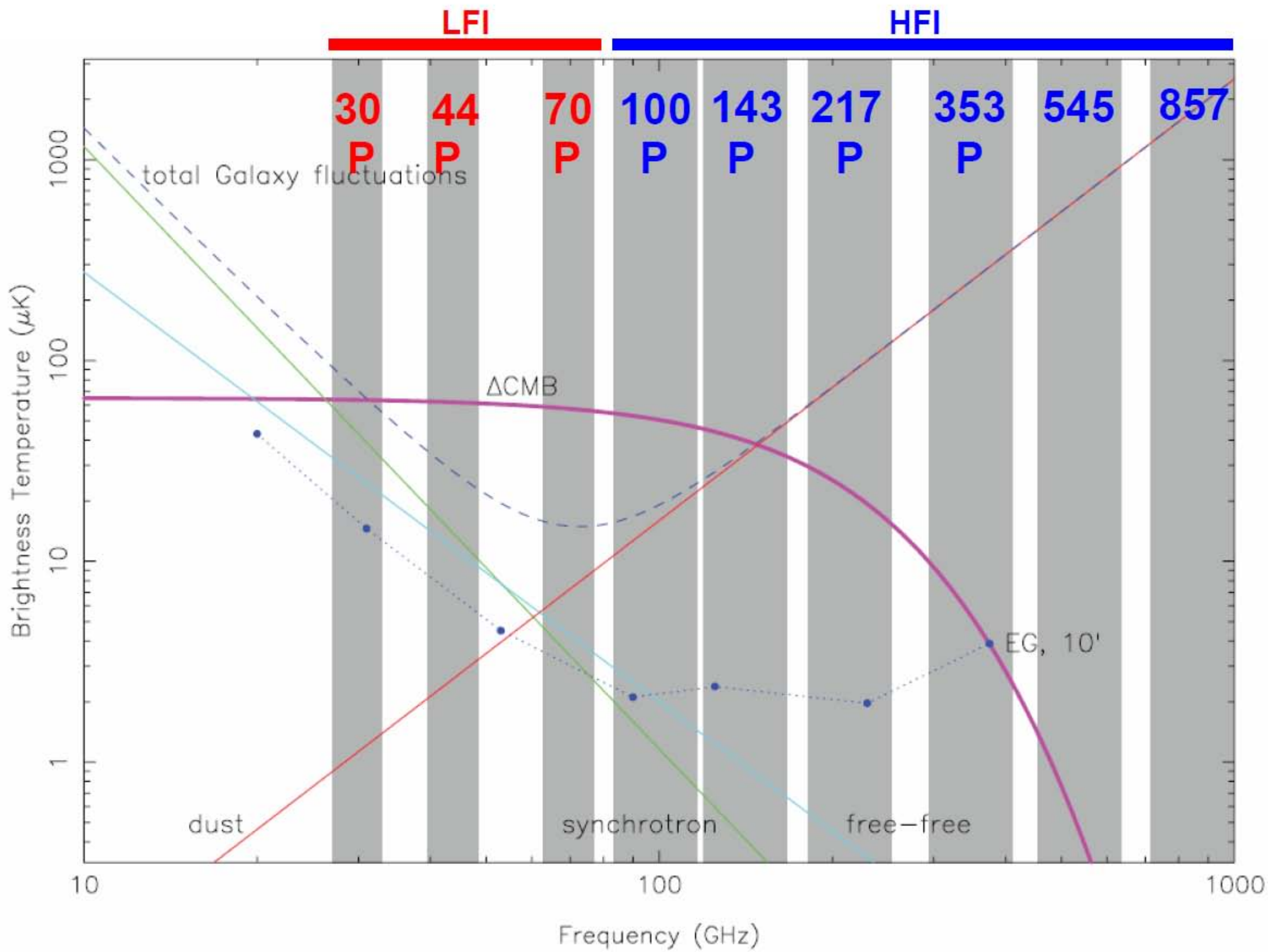
LFI
HFI
30 P
44 P
70 P
100 P
143 P
217 P
353 P
545
857
total Galaxy fluctuations
ΔCMB
EG, 10'
dust
synchrotron
free−free
Brightness Temperature (μK)
Frequency (GHz)
1
10
100
1000

Planck – HFI polarization sensitive focal plane

Ponthieu et al. 2010

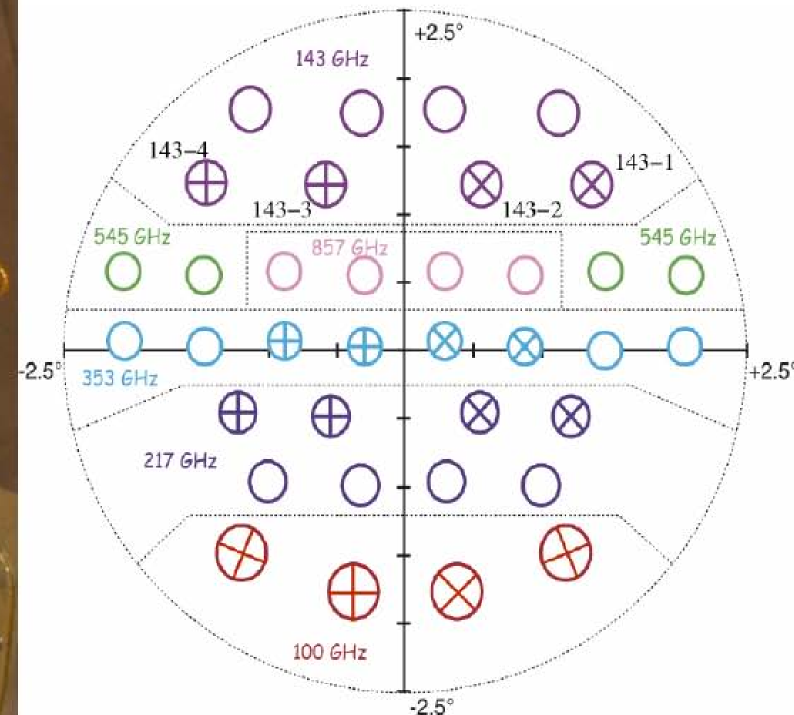

Scan direction

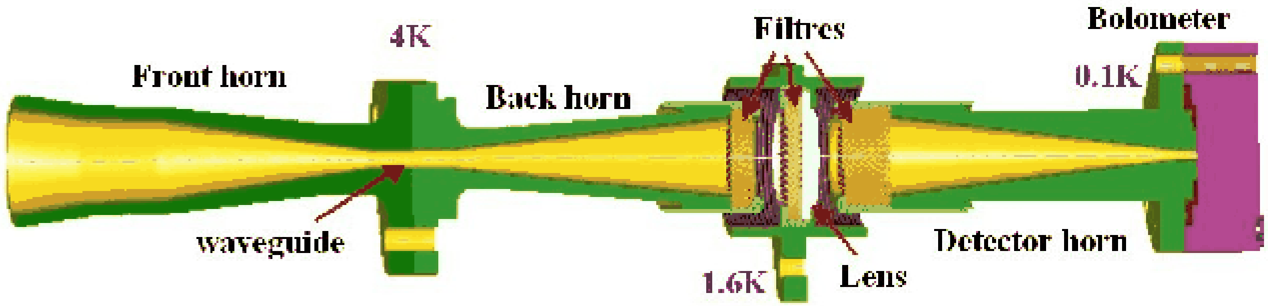

Front horn
4K
Back horn
Filtres
Bolometer
0.1K
waveguide
1.6K
Lens
Detector horn

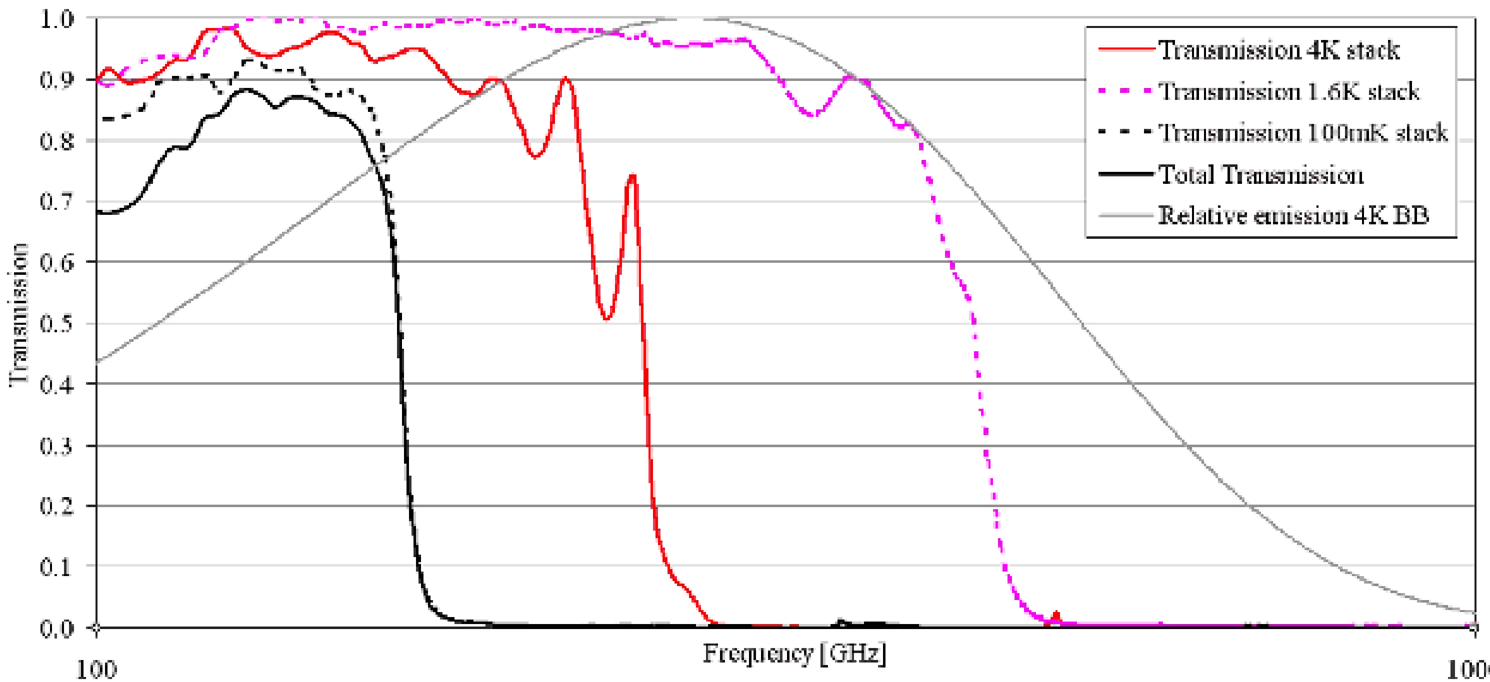

Transmission
Frequency [GHz]
100
1000
1.0
0.9
0.8
0.7
0.6
0.5
0.4
0.3
0.2
0.1
0.0
Transmission 4K stack
Transmission 1.6K stack
Transmission 100mK stack
Total Transmission
Relative emission 4K BB


HFI
Spider-web bolometers
Made in JPL
BOOMERanG 1998 (0.3K),
Archeops 2001 (0.1K),
….

Andrew Lange

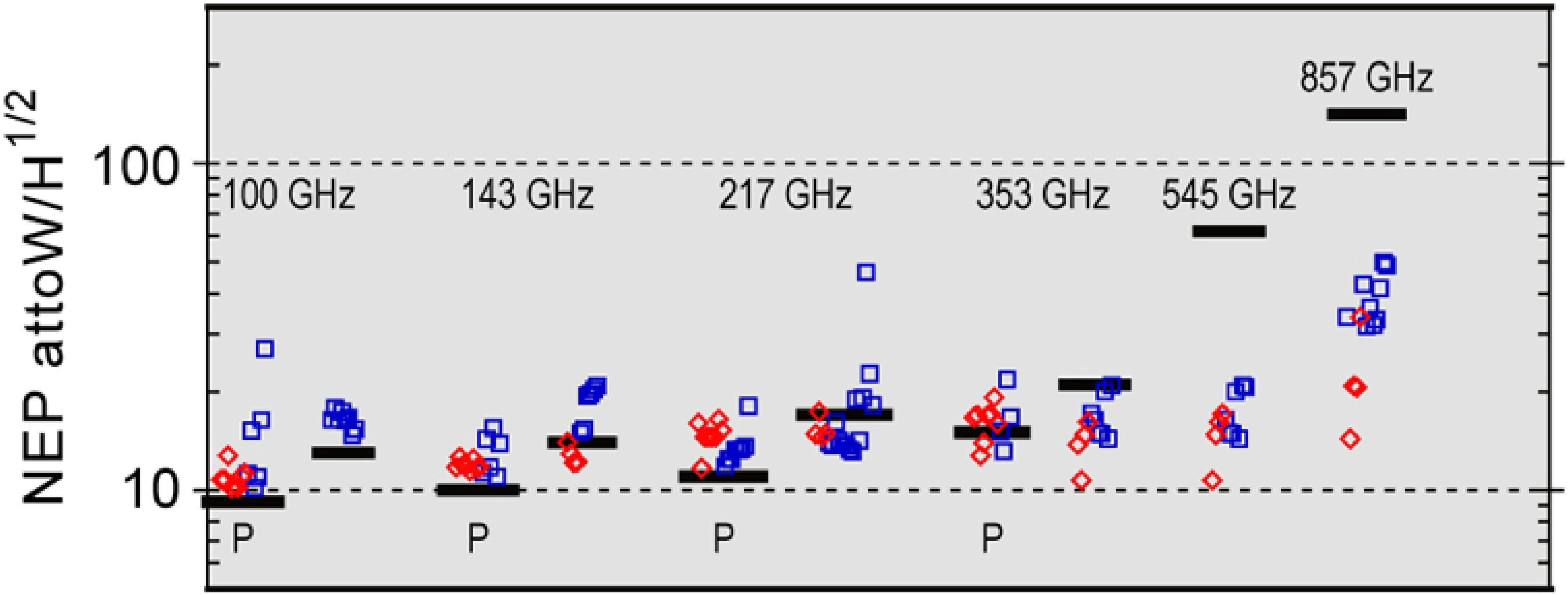

Measured dark noise equivalent power (NEP) of the focal plane detectors, including 6.5 nV / sqrt(Hz) amplifier noise at nominal bias. The open diamond symbols are the NEP for detectors installed in the focal plane. The open square symbols are the NEP of spare bolometers. The thick solid line segments indicate the photon background limit from a 35 K telescope and astrophysical sources in each band for a 30% bandwidth and 30% in band optical efficiency. Unpolarized detectors at 100 GHz were made and delivered but were replaced by polarized detectors. (from Holmes et al. (2008))

NEP_b = 15 aW/Hz$^{1/2}$ -> 70 μK/Hz$^{1/2}$

Total NET (bolo+photon) = 85 μK/Hz$^{1/2}$

HFI Ge bolometer preamp noise

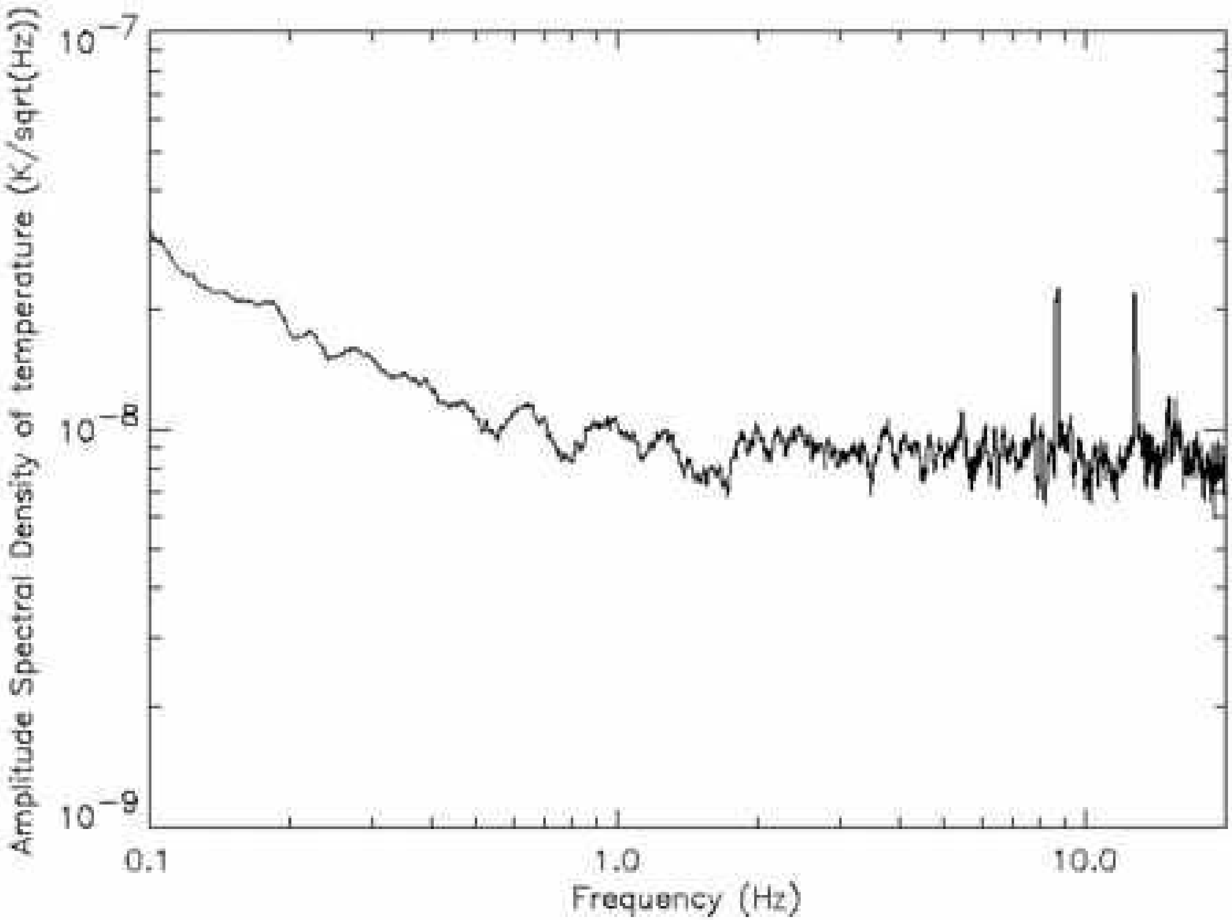

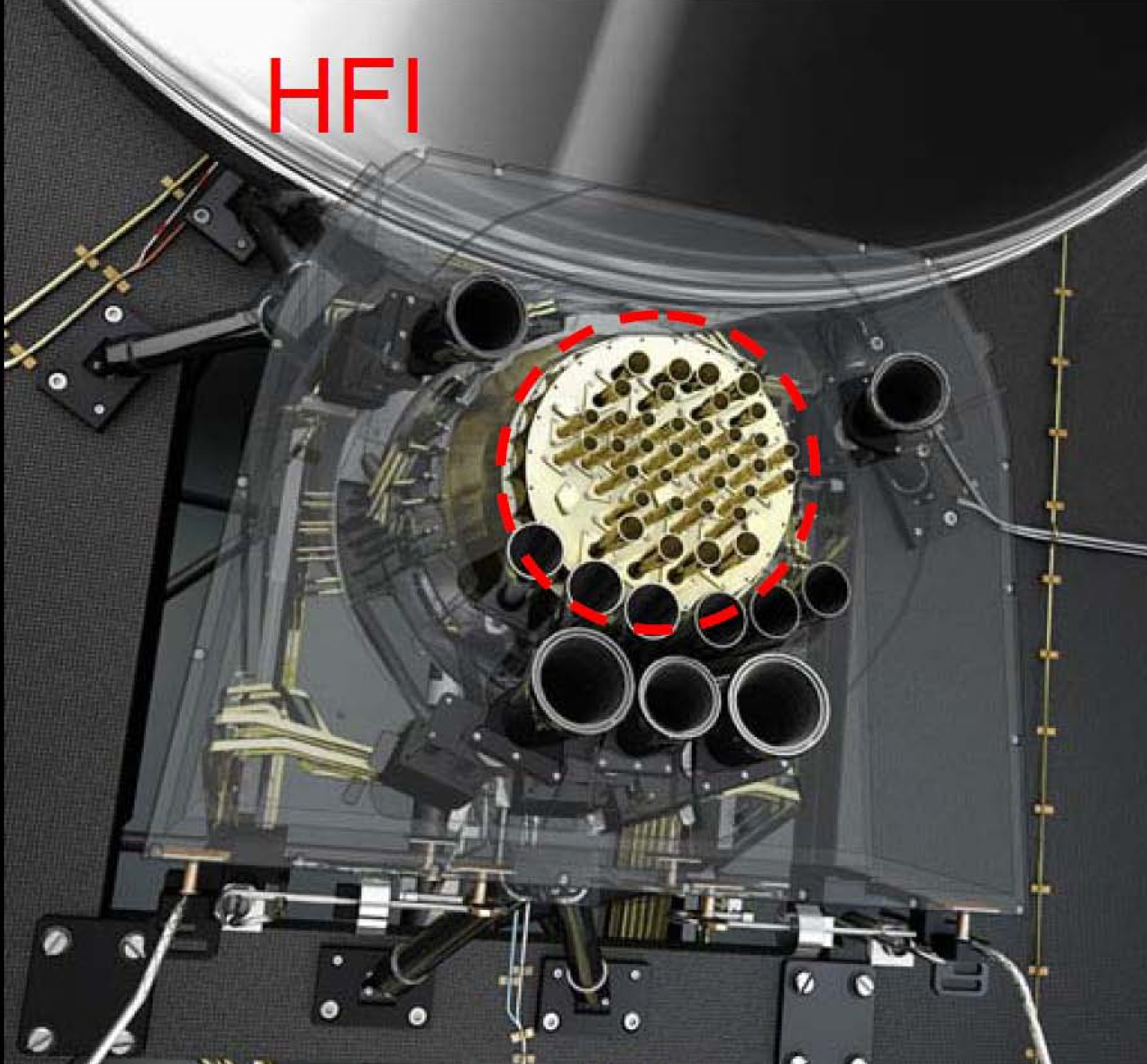
HFI

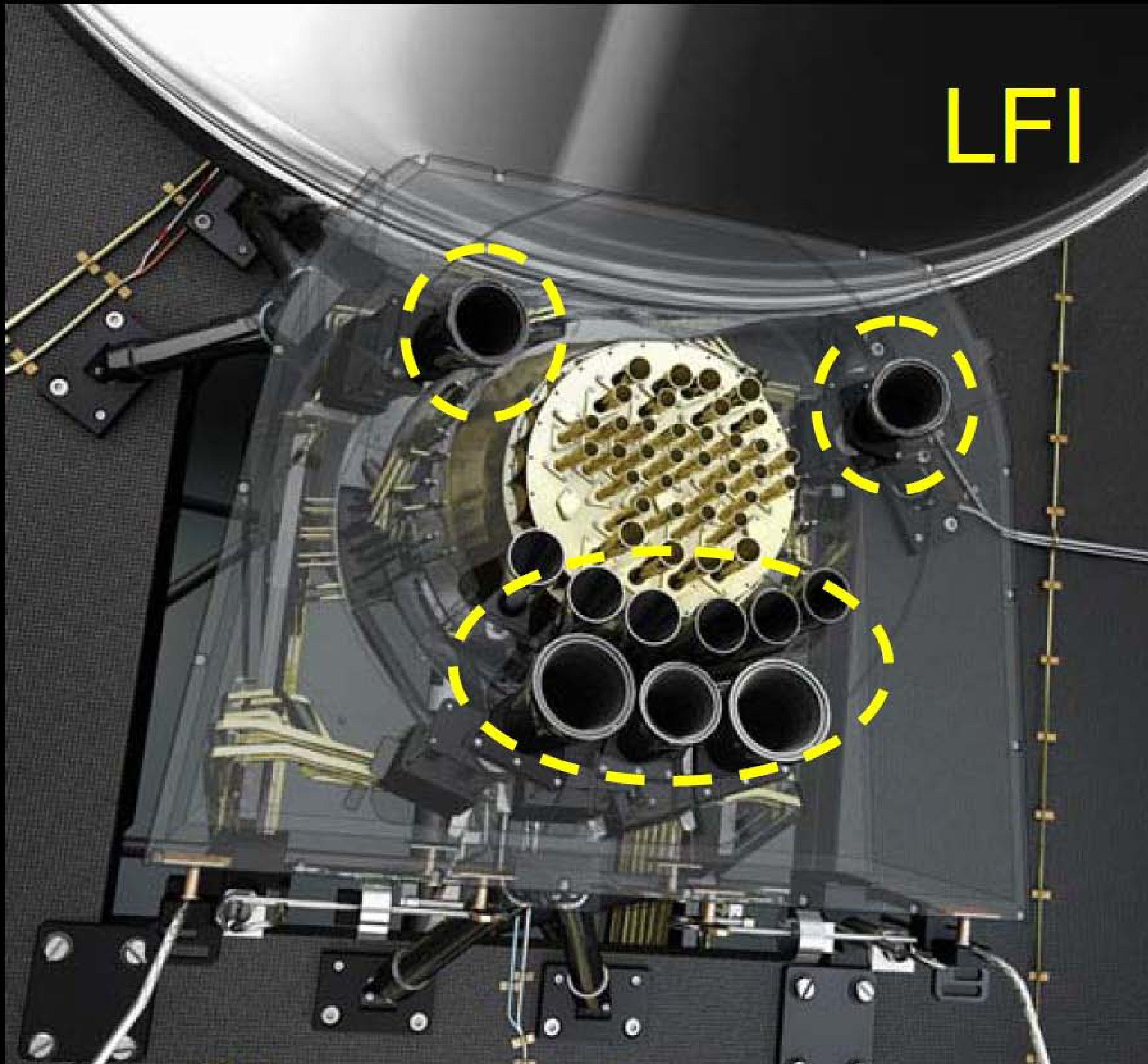
LFI

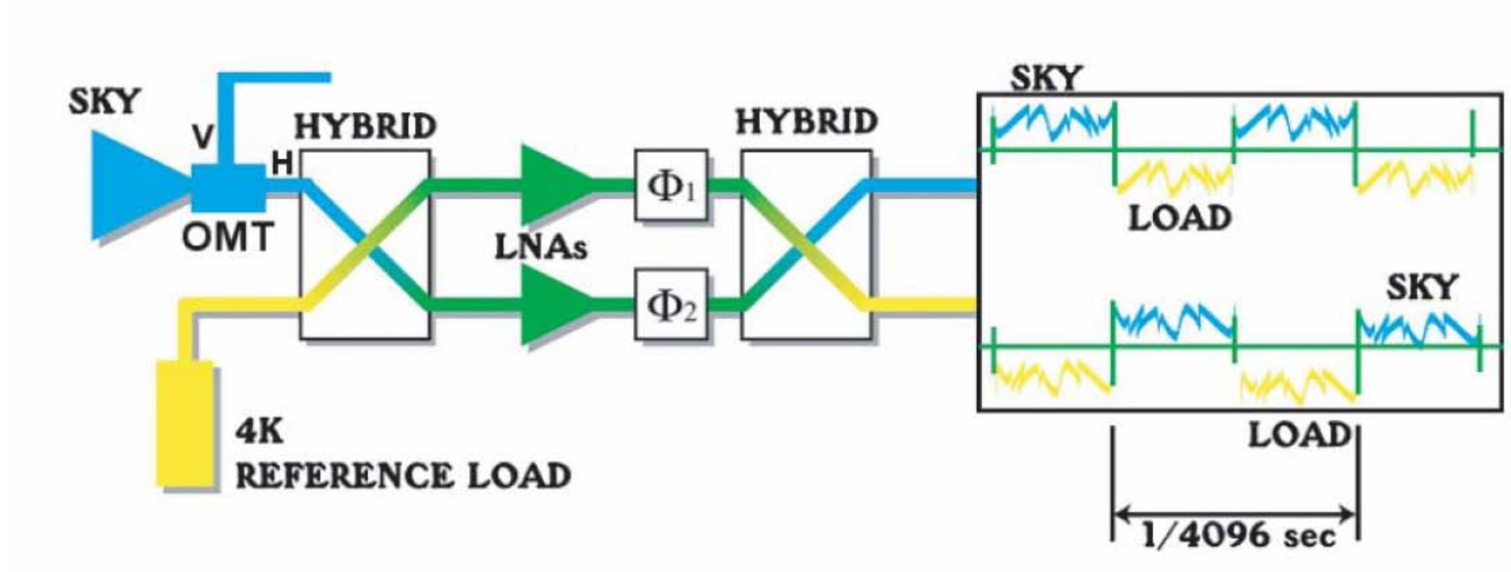

LFI
Pseudo-correlation
Differential radiometer
Measures I,Q,U
30, 44, 70 GHz

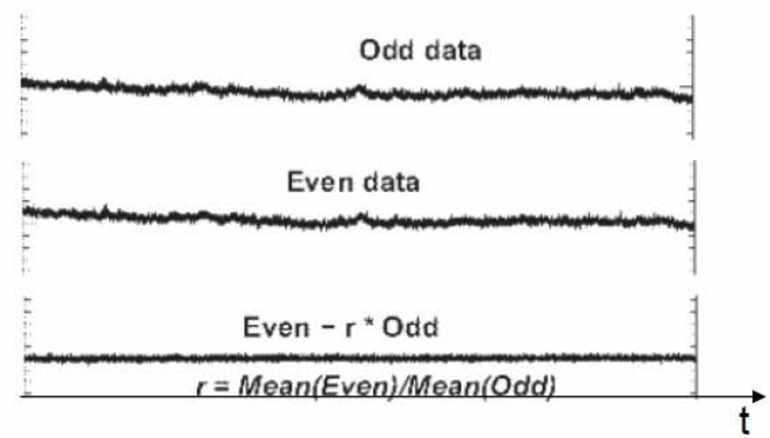

LFI noise before and after chops

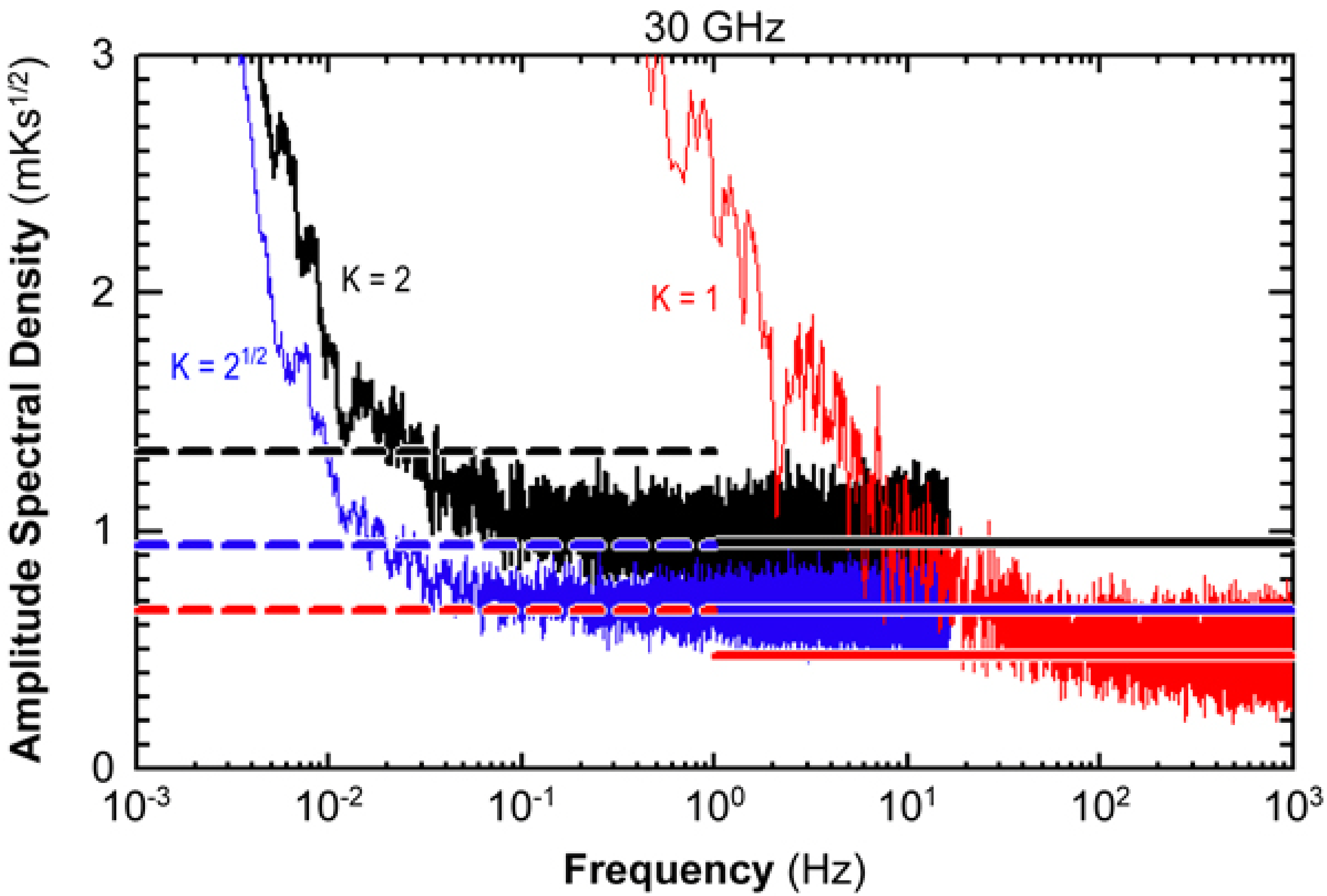


18
19
20

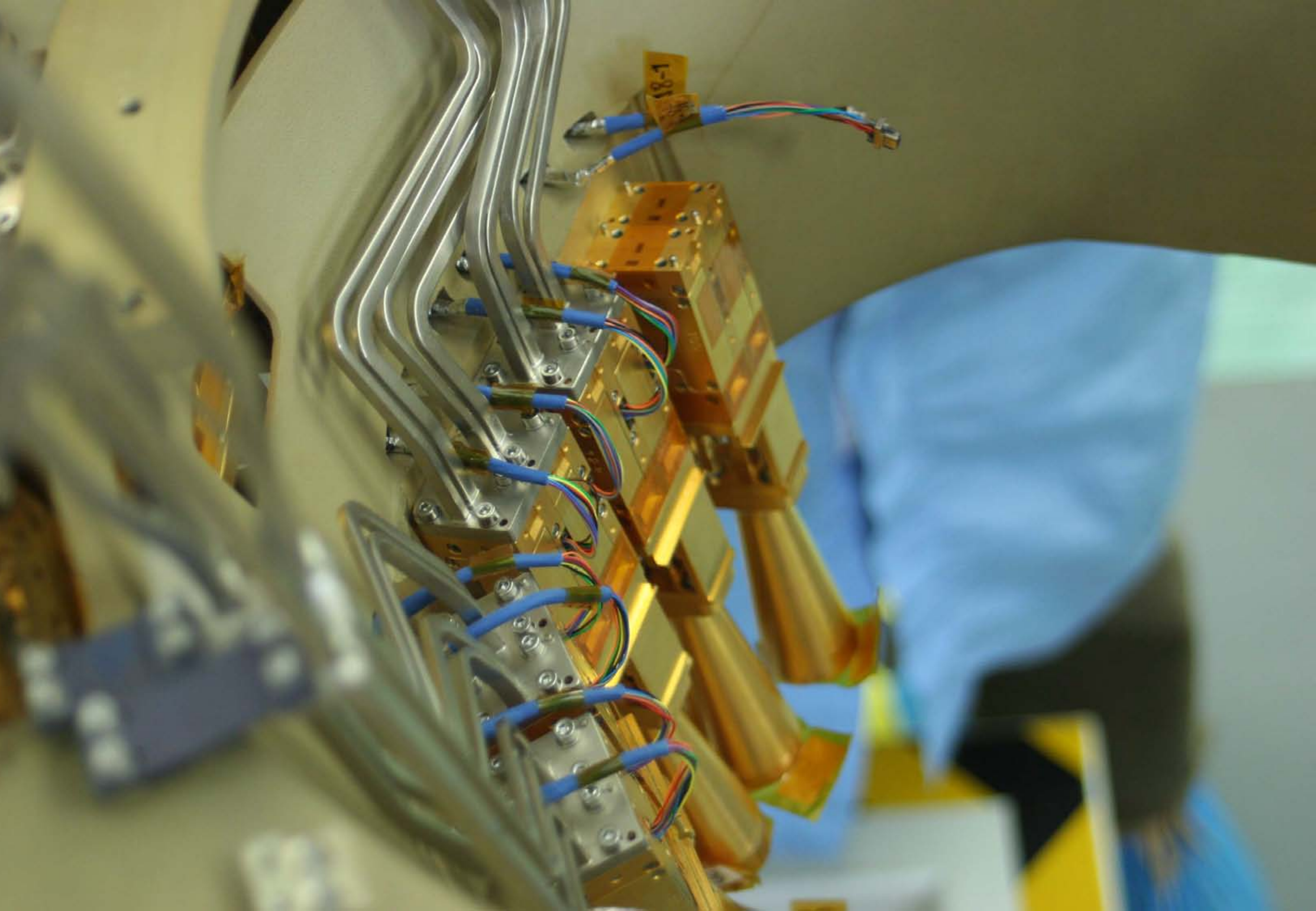

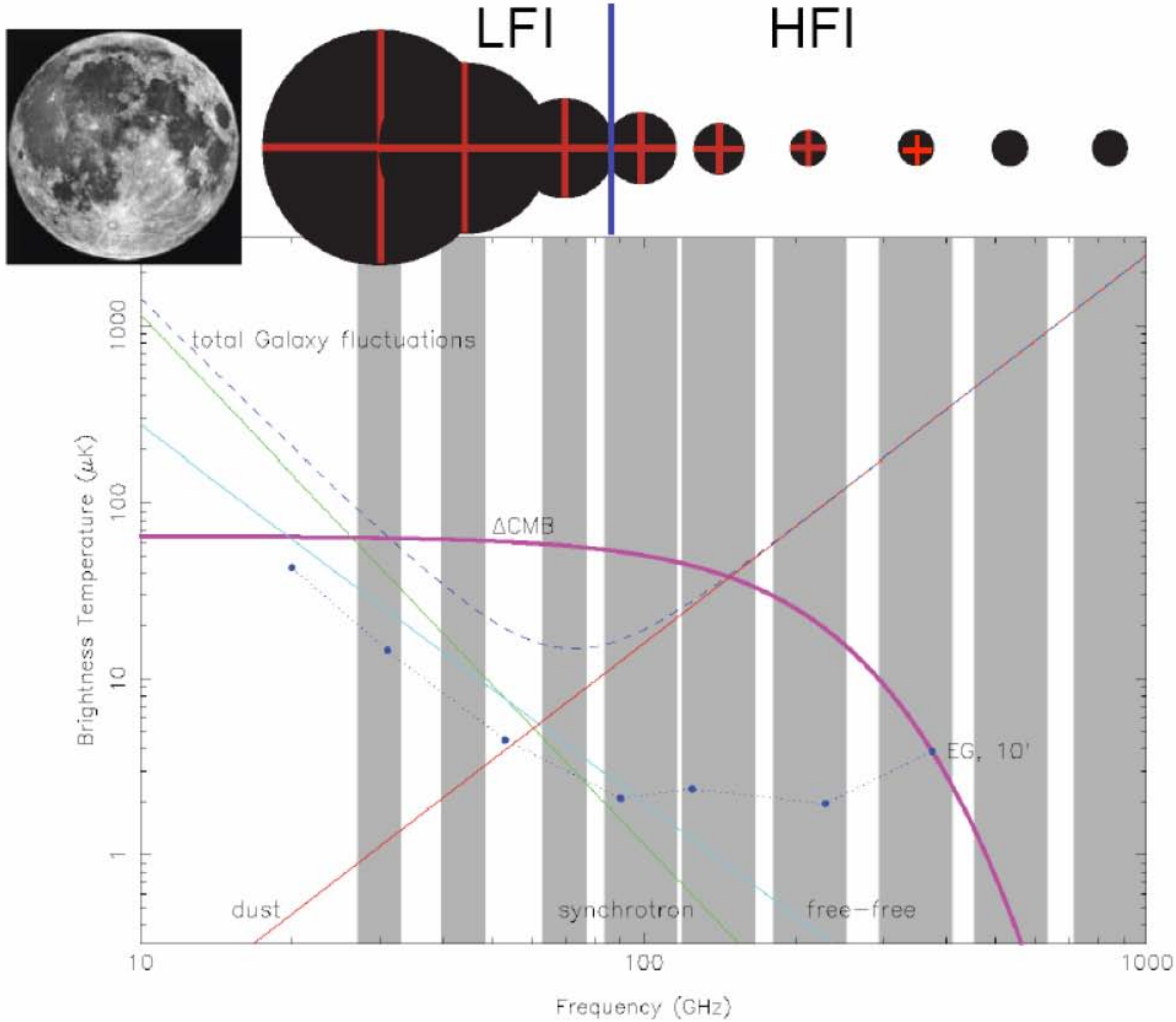
LFI
HFI
total Galaxy fluctuations
ΔCMB
EG, 10'
dust
synchrotron
free-free
Brightness Temperature (μK)
Frequency (GHz)
10
100
1000
1
10
100
1000

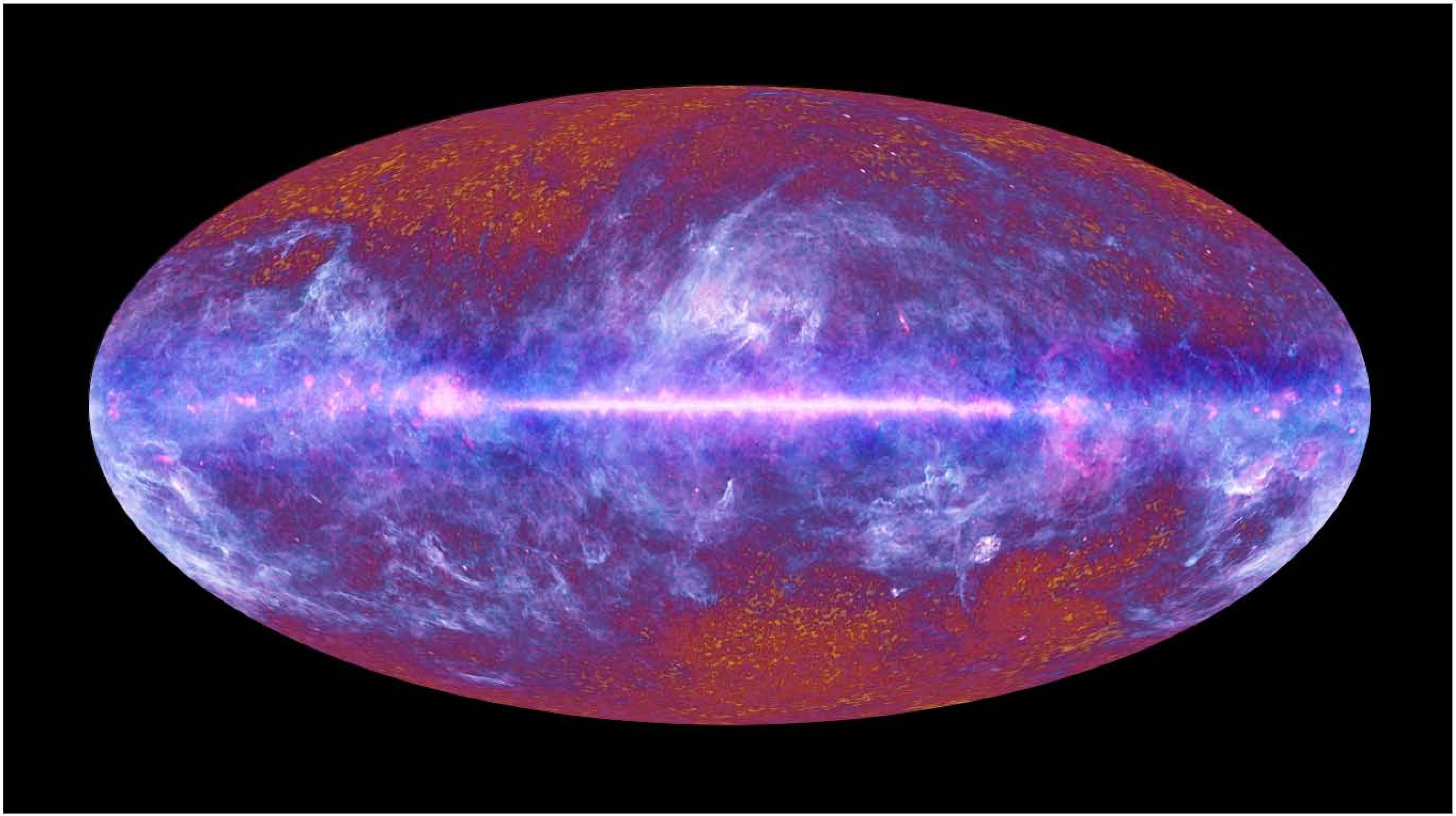

The Planck one-year all-sky survey

(c) ESA, HFI and LFI consortia, July 2010

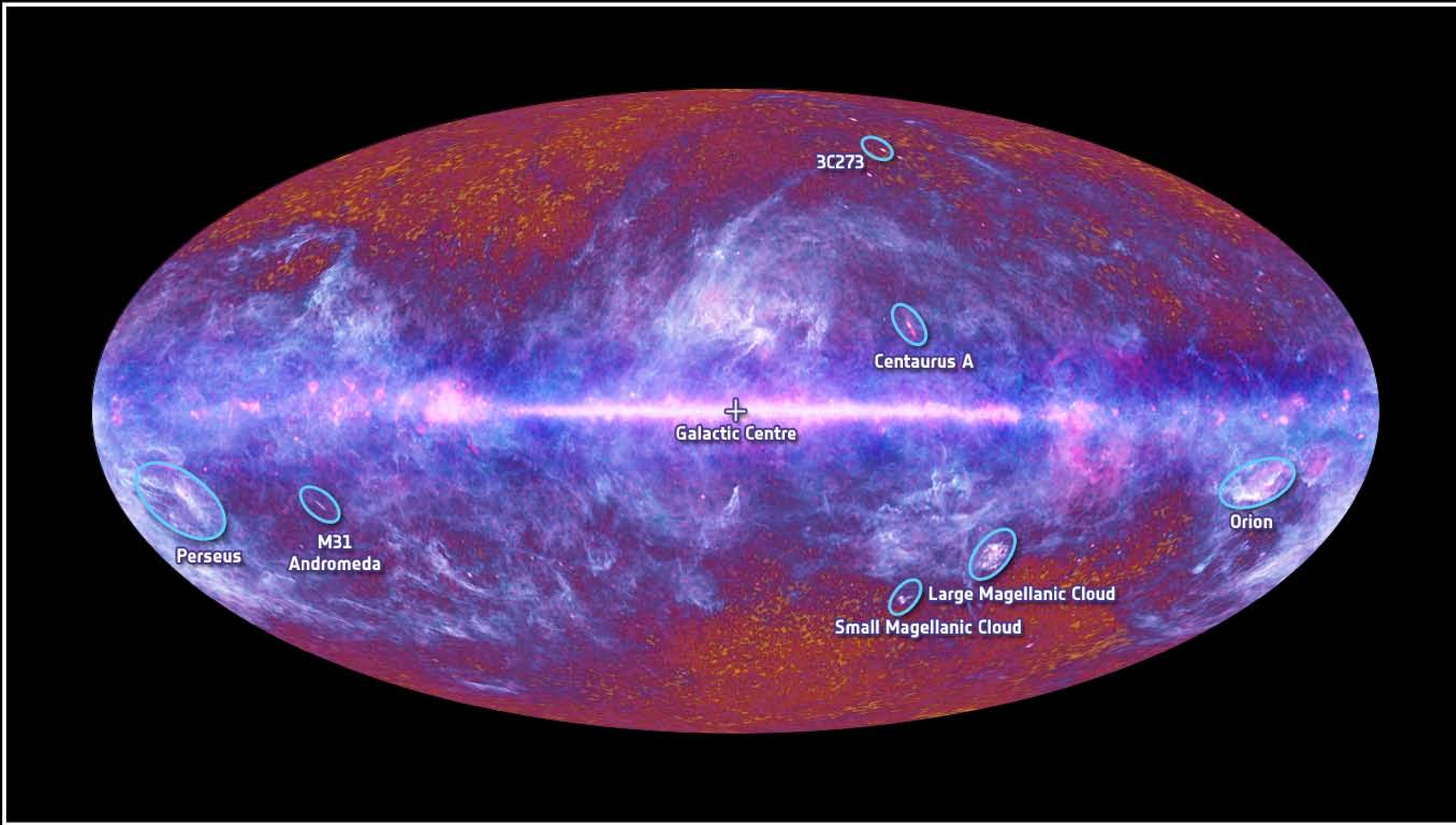

The Planck one-year all-sky survey

esa

(c) ESA, HFI and LFI consortia, July 2010

Inverse problems

'Most people, if you describe a train of events to them, will tell you what the result would be. They can put those events together in their minds, and argue from them that something will come to pass. There are few people, however, who, if you told them a result, would be able to evolve from their own inner consciousness what the steps were which led up to that result. This power is what I mean when I talk of reasoning backwards, or analytically.' · · · '· · · the grand thing is to be able to reason backwards. That is a very useful accomplishment, and a very easy one, but people do not practise it much. In the every-day affairs of life it is more useful to reason forwards, and so the other comes to be neglected. There are fifty who can reason synthetically for one who can reason analytically.'
(Sherlock Holmes in 'A Study in Scarlet')

Image space, data space, and noise

data d, image x, measurement noise n, forward map A

$$d = Ax + n$$

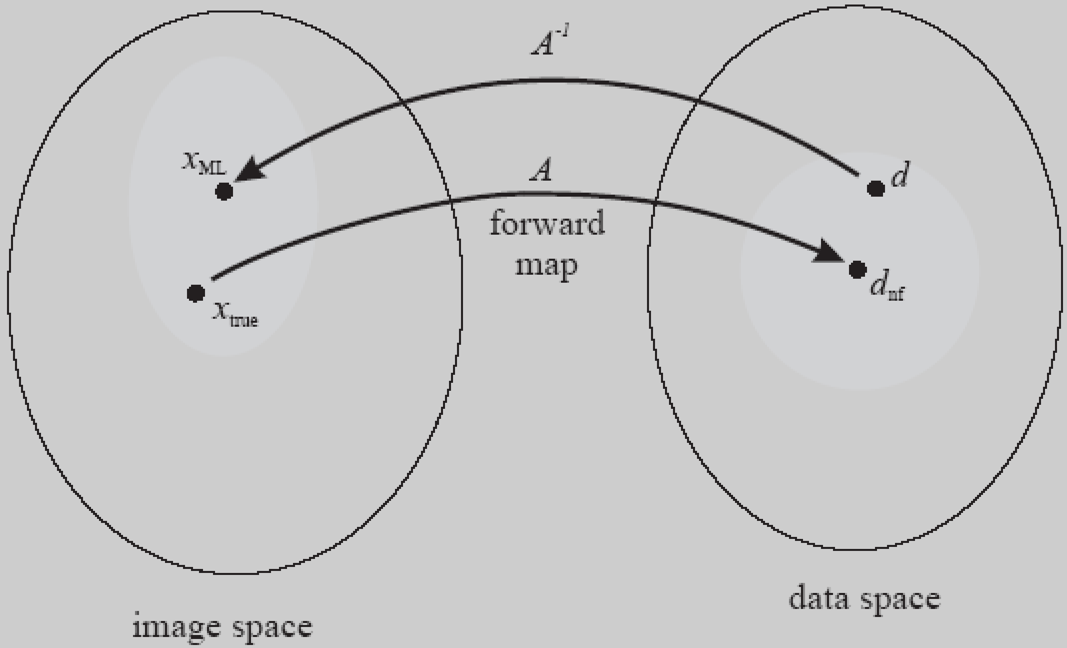

Inverse not unique

Actually a range of feasible images each being consistent with the measured data

Straightforward inversion of the noisy data d, is generally a terrible estimate

Stochastic model of an inverse problem

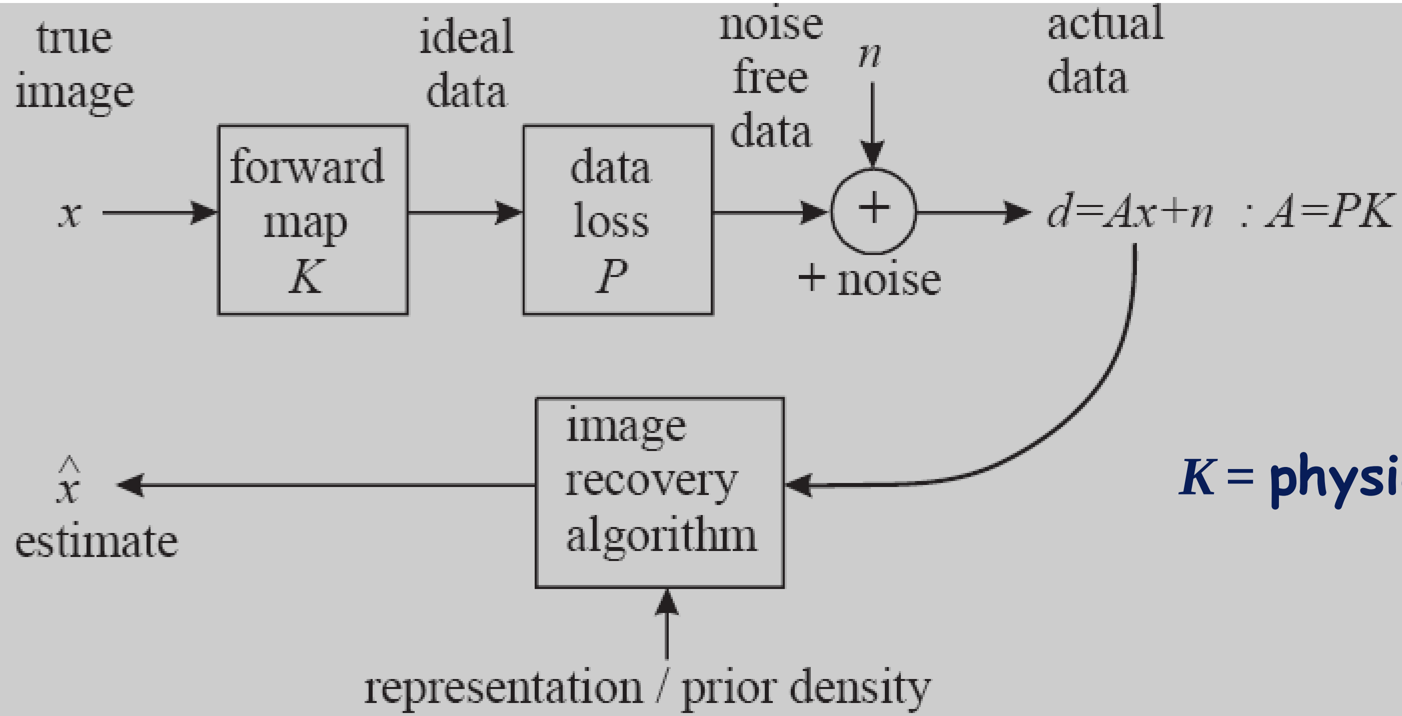

***K* = physics solution**

simulations help

if $n \sim f_N(\cdot)$ $\quad$ $\Pr(d|x,m) = f_N\left(d - Ax\right)$

Posterior distribution for x conditional on d

$$\Pr\left(x|d,m\right) = \frac{\Pr\left(d|x,m\right)\Pr\left(x|m\right)}{\sum\limits_{x \in X} \Pr(d|x,m)\Pr\left(x|m\right)} \qquad \text{(Bayes' rule)}$$

Parametric inversion

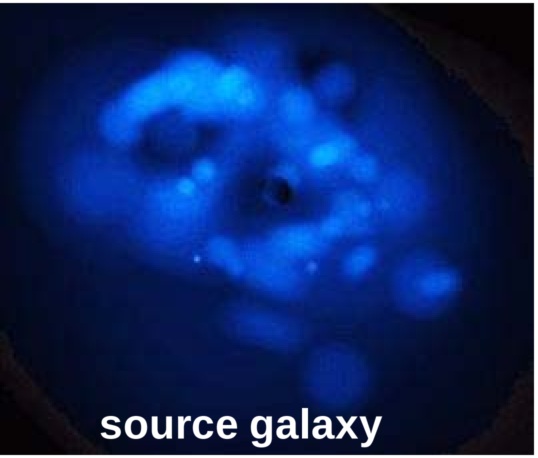

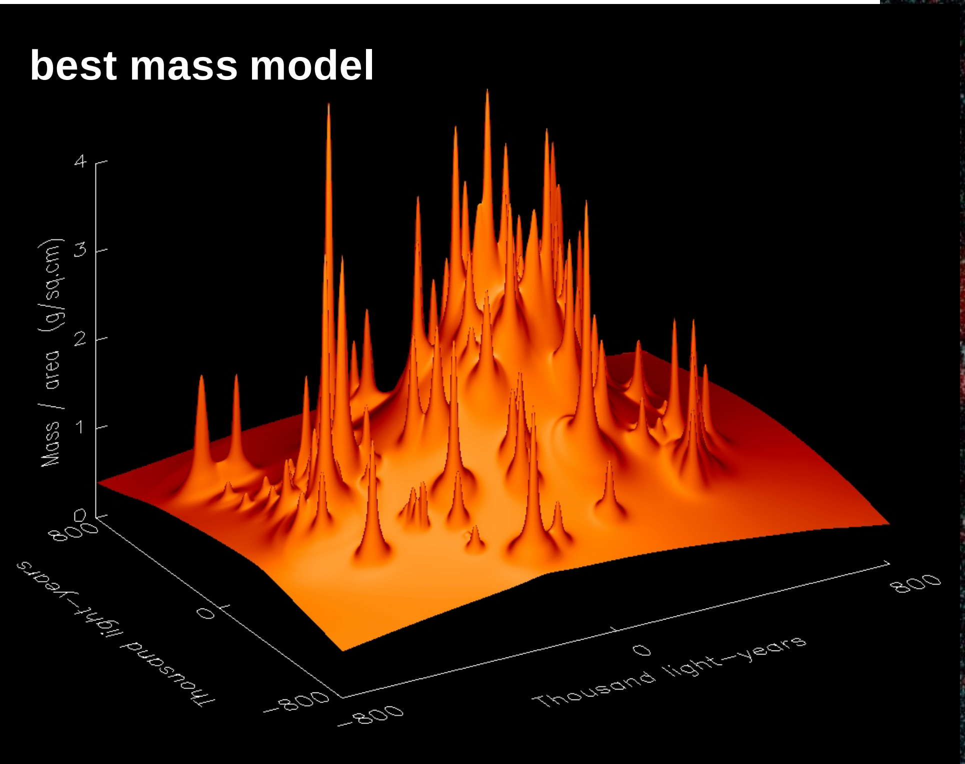

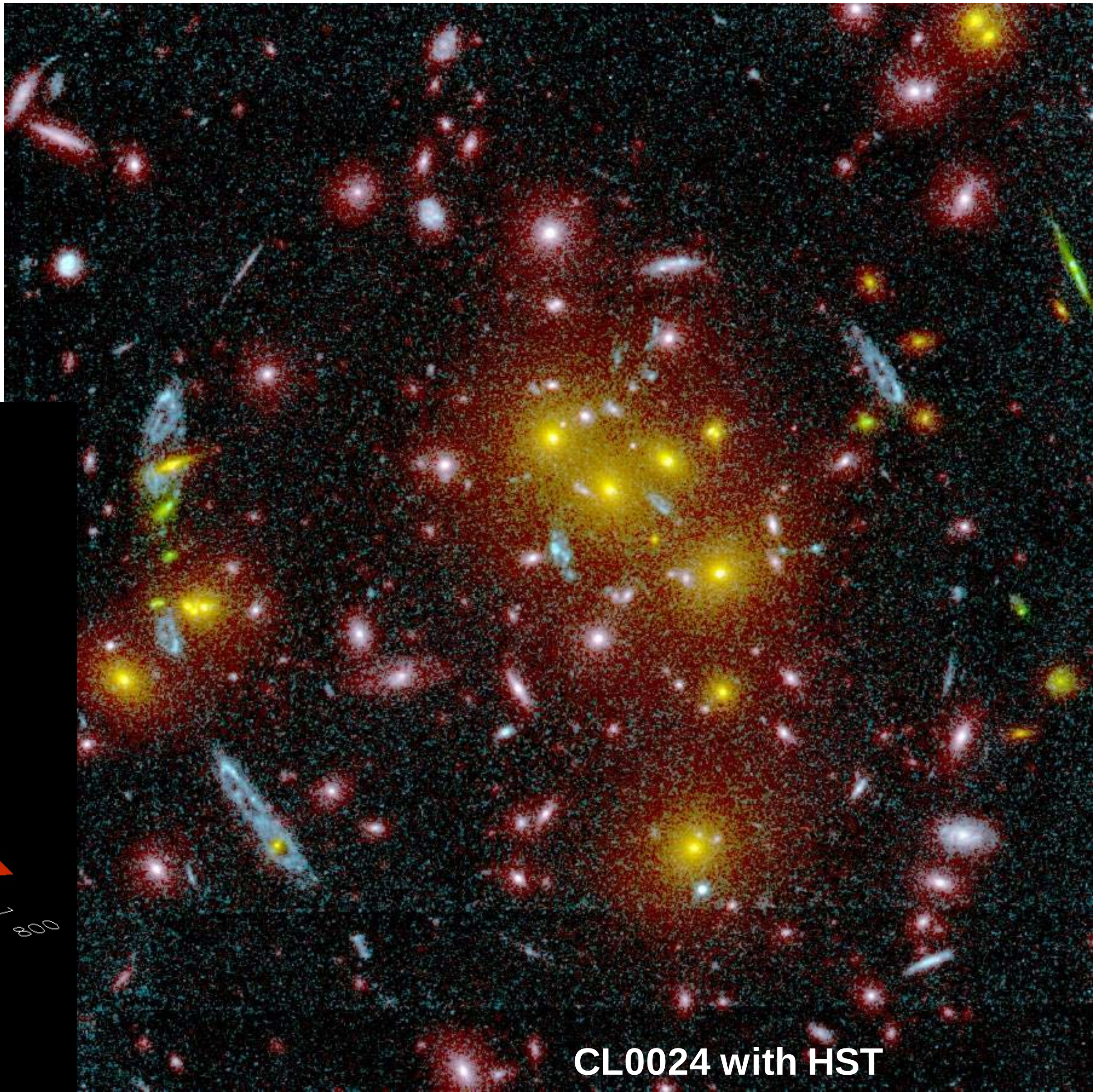

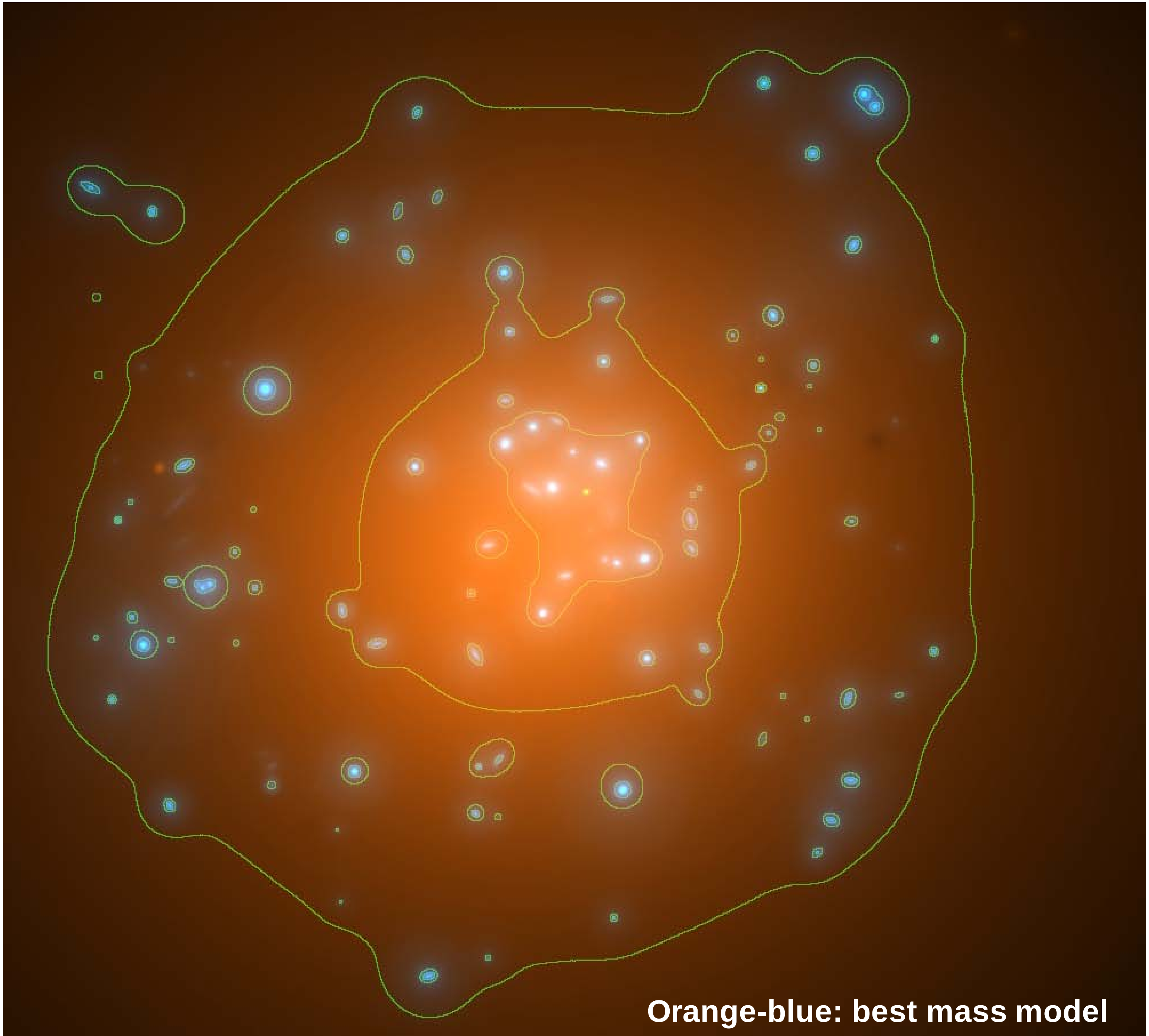
Orange-blue: best mass model

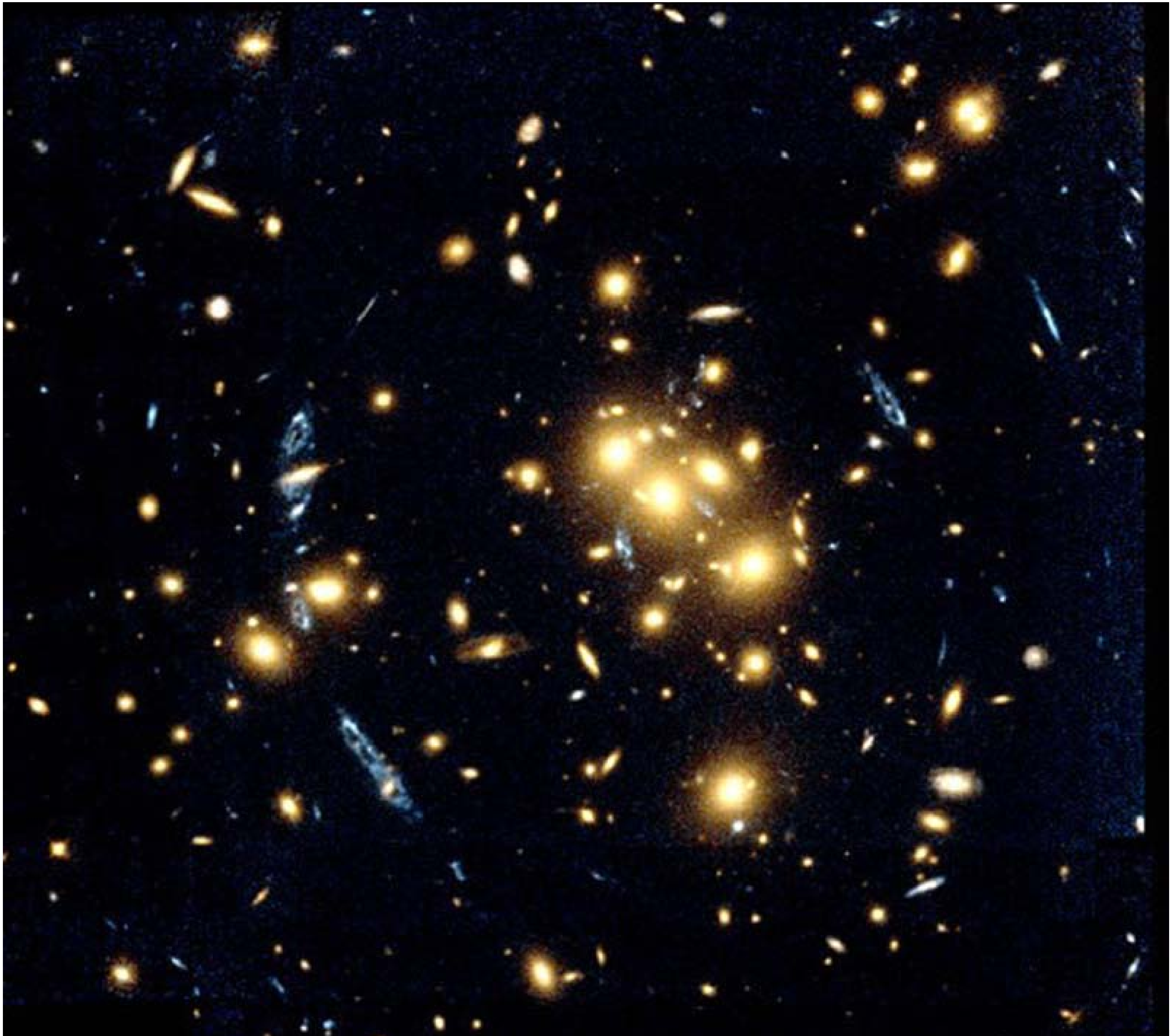

Simulations!

Simulations play a key role in regularized inverse solutions. Start with model of entire imaging process. Prior: chose classes of object images. Convolve with model. Select appropriate restoration method. Optimize inverse solution via regularization parameter.